

## Master Thesis

# Development of an Automatic IMU Calibration System

Spring Semester 2011

**Supervised by:**

Prof. Dr. R. Y. Siegwart  
S. Leutenegger  
Dr. S. Bouabdallah

**Author:**

Benjamin Peter



# Abstract

The goal of this thesis was to develop a device that simplifies and speeds up the calibration process of the accelerometers and gyroscopes on the Inertial Measurement Unit (IMU) developed by the Autonomous Systems Lab (ASL) at the ETH Zurich. A mechanical gimbal system with three actuated degrees of freedom has been designed and built. It is able to completely calibrate the IMU without any intermediary user manipulations, i.e. without the need to reposition it manually during the calibration process.

For the accelerometers, the calibration is done by positioning the IMU to known orientations and for the gyroscopes by rotating the IMU at several constant speeds around specified axes. Based on these measurements, the optimal parameters for the sensor error model are calculated using linear least squares. A set of trial calibrations were conducted and their results were evaluated.

To further simplify the user interaction with the developed calibration system, a graphical user interface was programmed and a manual was written.

The presented system could potentially be adapted for other, similarly sized IMUs.



# Acknowledgements

Many thanks go to my tutor Prof. Roland Siegwart and to Stefan Leutenegger and Dr. Samir Bouabdallah, who did an excellent job at supervising my master thesis. Very helpful technical advice was given by Markus Bühler and Dario Fenner at the ASL workshop. I am grateful for their time and for the manufacturing of all the milled and turned parts.

I owe a lot of credit for the design of the electronics to the experience and skill of Thomas Baumgartner, especially for the development of the PCB. I thank Stefan Bertschi for lending me a lot of lab equipment and for setting up the computer and Martin Schmid for helping me with the CAD software custom settings and templates.

I am thankful for the Legged Locomotion team with David Remy, Marco Hutter and Markus Höpflinger and for Andreas Breitenmoser for their advice regarding the motors and controllers and the software interface with Matlab.

Last but not least, I would like to thank Janosch Nikolic for lending me his IMU several times and Sammy Omari for his advice and for flashing IMUs for me on many occasions.



# Contents

<b>Abstract</b>	<b>i</b>
<b>1 Introduction</b>	<b>1</b>
1.1 Motivation . . . . .	1
1.2 Existing Systems and Related Work . . . . .	1
1.3 Definitions . . . . .	4
1.4 Goal . . . . .	5
1.5 Concept Overview . . . . .	5
1.6 Outline of this Thesis . . . . .	7
<b>2 Calibration Concept</b>	<b>9</b>
2.1 Outline . . . . .	9
2.2 Sensor Error Model . . . . .	9
2.3 Algorithm . . . . .	10
2.4 Rotation Schedule . . . . .	12
<b>3 Mechanical Design</b>	<b>15</b>
3.1 Overview . . . . .	15
3.2 Gimballs . . . . .	15
3.3 Shafts . . . . .	17
3.4 Base . . . . .	18
3.5 Actuation . . . . .	19
<b>4 Electronics</b>	<b>21</b>
4.1 Wiring . . . . .	21
4.2 Motor Controller . . . . .	21
4.3 PCB . . . . .	22
<b>5 Software</b>	<b>23</b>
5.1 Motor Control . . . . .	23
5.2 IMU Communication . . . . .	23
5.3 GUI . . . . .	23
<b>6 Calibration Procedure and Test Results</b>	<b>27</b>
6.1 Calibration Procedure . . . . .	27
6.2 Results . . . . .	27
6.3 Validation . . . . .	28
6.4 Accuracy of the Calibration System . . . . .	30
6.5 Repeatability . . . . .	30
<b>7 Conclusion</b>	<b>33</b>

<b>A Calibration System Manual</b>	<b>35</b>
A.1 Introduction . . . . .	35
A.2 Calibration System Overview . . . . .	36
A.3 Setup . . . . .	36
A.4 Calibration Procedure . . . . .	38
A.5 GUI Features . . . . .	40
A.6 Technical Data . . . . .	43
A.7 Maintenance and Handling Remarks . . . . .	49
<b>B Part List</b>	<b>50</b>

# Chapter 1

## Introduction

### 1.1 Motivation

An *Inertial Measurement Unit* (IMU) consists of a cluster of sensors, including accelerometers and gyroscopes that is used to determine the attitude of a body. Many contemporary systems heavily rely on IMUs for their navigation. Most prominently, IMUs are found on flying platforms, both fixed- and rotary-wing aircraft. Especially Micro Aerial Vehicles (MAV) and other Unmanned Aerial Vehicles (UAV) are in need for a compact device providing attitude information.

However, an IMU has to be calibrated before it can be put into operation. Calibration is necessary, because the sensor sensitivity axes usually do not coincide exactly with the body frame axes. This is due to manufacturing imperfections when soldering the sensors onto the board as well as imperfections of the sensors themselves. This may also include non-orthogonality of the sensitivity axes in addition to simple misalignment, especially if a cluster of one-axis sensors is used. As actual scale and bias values usually differ from the nominal values, they have to be determined, too. The calibration process requires a mechanical platform to precisely manipulate the IMU. A minimum of one actuated degree of freedom is needed to calibrate the gyroscopes. However such a system requires extensive and tedious user manipulation, as the IMU has to be repositioned several times. Thus, it is desirable to have a three degrees of freedom platform able to rotate the IMU around arbitrary axes in space, minimising the necessary user interactions.

The *Autonomous Systems Lab* (ASL) at the ETH Zurich has developed a small-sized low-cost IMU [1]. It is depicted in figure 1.1. Until now, the ASL IMU has been calibrated with the help of a very simple setup using only a single motor. It would be advantageous to reduce the effort of calibration by developing a compact, easy to use calibration system.

### 1.2 Existing Systems and Related Work

Commercially available calibration systems<sup>1</sup> (figure 1.2) and rate tables usually are very expensive and large.

To the author's knowledge, there is no commercial mechanical system specifically designed for the calibration of small-sized IMUs. There are systems that could be used or adapted to perform the task, but they all have drawbacks. For example limited accuracy and rotation range (angle limitations on all rotational degrees of

---

<sup>1</sup>Acutronic, <http://www.acutronic.com/1/products.html>



Figure 1.1: The IMU developed by the Autonomous Systems Lab.



Figure 1.2: Commercial calibration system from Acutronic.

freedom not allowing continuous rotation) due to the mechanical design<sup>2,3</sup> or simply due to their large size and high cost, as stated before. Madgwick even used a camera pan-tilt platform<sup>4</sup> for a calibration in a feasibility study [2] (figure 1.3).

Other examples of platform concepts are the variable-geometry truss and the carpal wrist [3]. They both feature a frame actuated by several linear actuators. The kinematics and control of such platforms is quite complex, as is its construction. The Virginia Tech Carpal Wrist [3] uses GPS to improve the control, which is of course not available indoors, unfortunately. An advantage of these platforms is that they are capable of producing linear motion. Thus, it may be possible to generate accelerations in excess of 1g which can otherwise only be generated with centripetal acceleration, if needed.

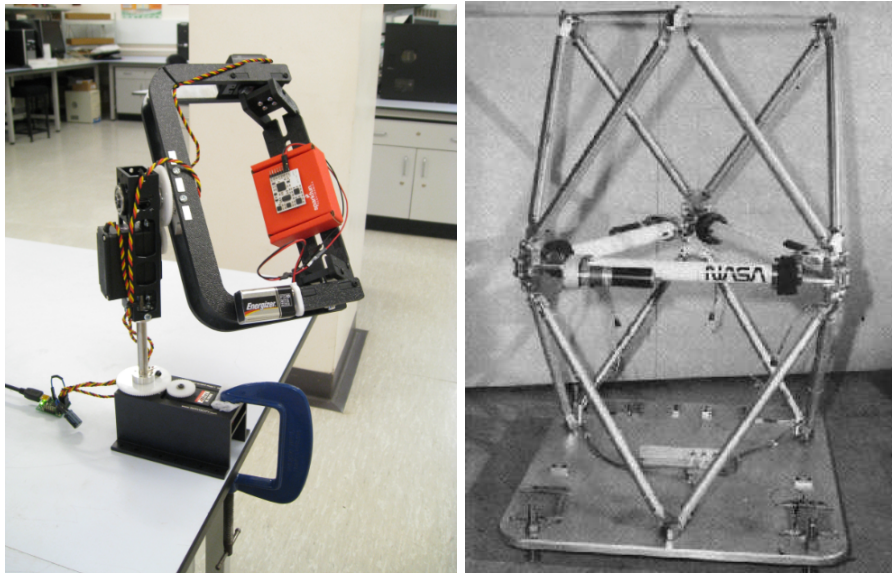


Figure 1.3: Left: pan-tilt camera platform used for calibration by Madgwick [2]. Right: Double-Octahedral Variable Geometry Truss [3].

Calibration platforms using linear actuators are not very common, most platforms consist of a gimbal system using rotational actuators [4] or even just one rotating panel [5] (figure 1.4). The number of rotational degrees of freedom usually ranges from one to three. These platforms use gravity to calibrate the accelerometers.

An entirely different approach is presented in [6]. No mechanical platform is used whatsoever. Instead, the IMU is moved manually. This movement is tracked by an optical system with the help of LEDs placed on the IMU. Given this kinematics information and sensor error models, the calibration parameters are calculated using a non-linear least squares algorithm. A disadvantage of this method is that the individual sensors cannot be calibrated separately, or only approximately separately, due to the imprecision of the manual movement.

<sup>2</sup>The Modal Shop, Turnkey Accelerometer Calibration Workstation,  
<http://www.modalshop.com/calibration.asp?ID=77>

<sup>3</sup>Accelerometer, magnetometer & gyroscope calibration,  
<http://www.youtube.com/watch?v=XqQCbknCVYI>

<sup>4</sup>Servocity, <http://www.servocity.com/>

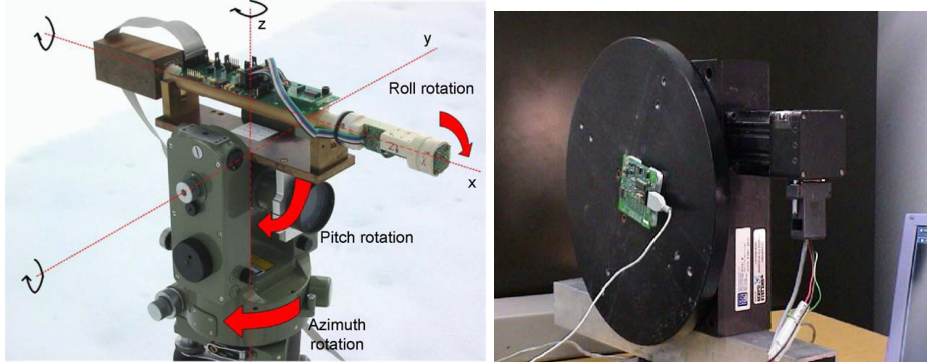


Figure 1.4: Left: calibration device by Včelák et al. [4]. Right: rotation panel by Park and Gao [5].

## 1.3 Definitions

### 1.3.1 Accelerometer, Gyroscope, IMU

An *accelerometer* measures accelerations superimposed with gravitational acceleration with respect to inertial space, i.e. *specific force* [7].

A *gyro*, short for *gyroscope*, measures the rotation rate relative to an inertial frame [7].

An *Inertial Measurement Unit (IMU)* comprises of a cluster of at least three accelerometers and three gyros. This allows to measure all six degrees of freedom – three translation and three rotation – of an arbitrary motion in three-dimensional space [7]. Usually, IMUs have several additional sensors to improve the accuracy of the overall measurement through sensor fusion. Examples are magnetometers, temperature sensors and pressure sensors.

### 1.3.2 Tait-Bryan Angles

*Tait-Bryan Angles*, also called *Cardan Angles*, are used to describe the orientation of a body in 3D-space. There are three angles: *roll*, *pitch* and *yaw*. They correspond to the gimbal angles of a three-axes gimbal system.

The sequence of rotations is zyx (yaw-pitch-roll), i.e. the system is first rotated about the z-axis by an angle  $\psi$ , then around the current y-axis by  $\theta$  and finally around the current x-axis by  $\varphi$ . A visualisation of the Tait-Bryan angles is shown in figure 1.5.

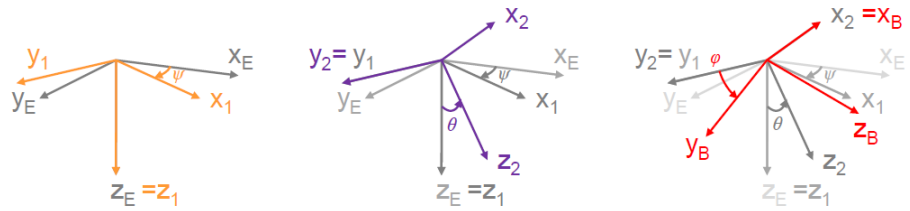


Figure 1.5: Tait-Bryan angles. Body frame with respect to an inertial frame. The image is courtesy of Stefan Leutenegger.

The resulting transformation matrix is calculated as shown in equation (1.1).

$$R_{total} = R_z(\psi) \cdot R_y(\theta) \cdot R_x(\varphi) \quad (1.1)$$

A comprehensive collection of attitude representations and conversions between them can be found in [8].

### 1.3.3 Calibration

'Calibration is the process of comparing instrument outputs with known reference information and determining coefficients that force the output to agree with the reference information over a range of output values' [7].

### 1.3.4 Abbreviations

ADC	Analog-to-Digital Converter
ASCII	American Standard Code for Information Interchange
ASL	Autonomous Systems Lab
CAD	Computer-Aided Design
CAN	Controller Area Network
DOF	Degree of Freedom
EPOS	Easy to use Positioning System
ESD	Electrostatic Discharge
GPS	Global Positioning System
GUI	Graphical User Interface
IMU	Inertial Measurement Unit
LED	Light-Emitting Diode
MAV	Micro Aerial Vehicle
PCB	Printed Circuit Board
UART	Universal Asynchronous Receiver/Transmitter
UAV	Unmanned Aerial Vehicle
USB	Universal Serial Bus

## 1.4 Goal

The goal of this thesis is to simplify and speed up the calibration process of the accelerometers and gyroscopes on the ASL IMU [1]. The aim is to be able to completely calibrate the IMU without any intermediary user manipulations, most importantly without the need to reposition the IMU during the calibration process. As a guideline, a maximum of  $\pm 600\text{deg}/\text{s}$  should be achieved for rotational speeds and  $\pm 1g$  for accelerations.

## 1.5 Concept Overview

To achieve the stated goal, a three degrees of freedom mechanical system has been developed. It is capable of exciting any IMU sensitivity axis. See figure 1.6.

With the middle and inner gimbal, a specific input axis of the IMU can be selected. For the accelerometer calibration, the selected axis is aligned to the gravity vector and gravity is measured. For the gyro calibration, the selected axis is aligned to the rotation axis of the outer gimbal. This gimbal is then rotated and its constant rotational speed is measured. In order to use the same alignment for the calibration of both sensor types, the rotation axis of the outer gimbal has to be manually aligned to the gravity vector.

Note that in this system, the orientation of the inner gimbal - and the IMU - is easily described by *Tait-Bryan angles* (see section 1.3.2). In fact, the gimbal angles of such a system are the very definition of Tait-Bryan angles.

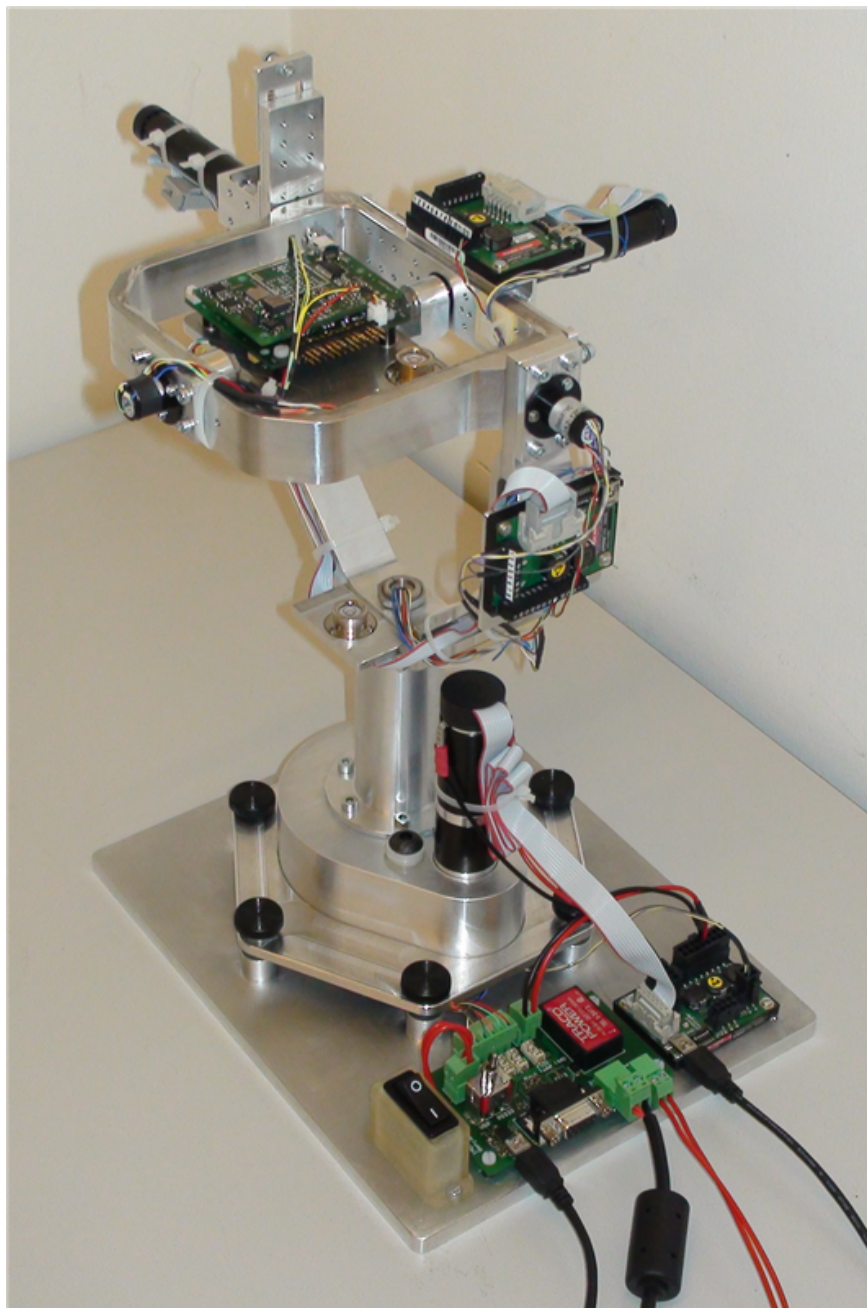


Figure 1.6: The IMU Calibration System. It has three independent gimbals. The IMU is attached to the inner gimbal.

## 1.6 Outline of this Thesis

First the concept of a calibration is discussed in chapter 2, including the implemented sensor error model and algorithm. In chapters 3, 4 and 5, the features of the developed calibration system are described. They include mechanical design, electronics and software.

A brief description of the whole calibration procedure and results from trial calibrations are presented in chapter 6.

In appendix A, a manual of the developed calibration system can be found. It comprises all necessary information to be able to set up the system and calibrate the IMU.

CAD drawings of all milled and turned parts designed for the system are given in appendix B.



# Chapter 2

## Calibration Concept

### 2.1 Outline

The calibration of the accelerometers is done by positioning the IMU to a set of known orientations and measuring gravity, more specifically the resulting reaction force. For the gyroscopes, the IMU is rotated at constant rotational speeds around a set of specified axes and these rotational speeds are measured. The chosen configurations are described in section 2.4.

At each configuration, a set of samples is taken for each sensor after waiting for it to settle.

Based on these measurements, the optimal parameters of the sensor model for the accelerometers and gyroscopes are calculated using a least squares algorithm.

The used sensor error model and its unknown parameters are described in section 2.2 and the calibration algorithm is discussed in section 2.3.

### 2.2 Sensor Error Model

The sensor model describes the process of measurement from the actual physical quantity to the sensor voltage output.

For both, accelerometers and gyroscopes, the same linear model is used. It accounts for *scale*, *misalignment*, *non-orthogonality* and *bias errors*. The described model is taken from [9] and [1], a similar model can be found in [10].

First, misalignment and non-orthogonality errors are dealt with.

Aligning the non-orthogonal sensor sensitivity axes to the orthogonal body frame coordinate axes requires a total of six angles [9], see figure 2.1. If the sensitivity axes differ only by small angles from the body frame axes, the measurements in sensitivity coordinates can be transformed into measurements in body frame coordinates as

$$s^B = Ts^S, \quad T = \begin{bmatrix} 1 & -\alpha_{yz} & \alpha_{zy} \\ \alpha_{xz} & 1 & -\alpha_{zx} \\ -\alpha_{xy} & \alpha_{yx} & 1 \end{bmatrix} \quad (2.1)$$

where  $s^B$  and  $s^S$  denote the measurement in body frame coordinates and IMU sensitivity coordinates, respectively.  $\alpha_{ij}$  is the rotation of the  $i$ -th sensor sensitivity axis around the  $j$ -th body frame axis, see figure 2.1.

A scaling matrix  $K$  and a bias vector  $b$  are introduced, defined as

$$K = \text{diag}(k_x, k_y, k_z), \quad b = [b_x \ b_y \ b_z]^T \quad (2.2)$$

where  $k_i$  and  $b_i$  are scaling and bias of the output of the sensor's  $i$ -th sensitivity axis.

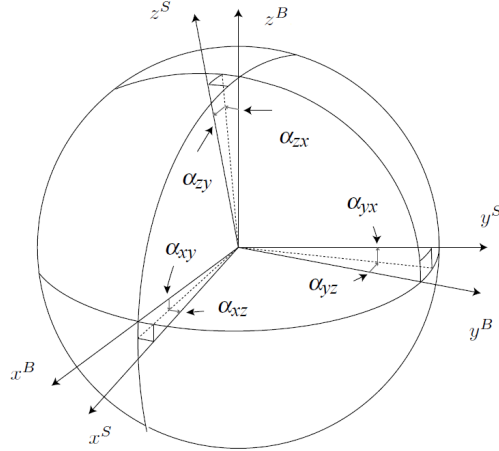


Figure 2.1: Sensor (accelerometer or gyroscope) sensitivity axes  $x^S, y^S, z^S$  and body frame coordinate axes  $x^B, y^B, z^B$ . The image is taken from [9].

Using  $s^S = T^{-1}s^B$  from equation (2.1), the sensor error model equation is

$$\begin{aligned} y &= Ks^S + b + \nu \\ &= KT^{-1}s^B + b + \nu \end{aligned} \quad (2.3)$$

where  $y$  is the sensor voltage output and  $\nu$  is the measurement noise.

The described sensor error model uses a total of twelve parameters: three for scale errors, three for bias errors and six for misalignment and non-orthogonality errors. They are:

$$\theta = [k_x \ k_y \ k_z \ b_x \ b_y \ b_z \ \alpha_{xz} \ \alpha_{xy} \ \alpha_{yx} \ \alpha_{yz} \ \alpha_{zx} \ \alpha_{zy}]^T \quad (2.4)$$

## 2.3 Algorithm

The calibration algorithm needs as inputs

- sample vector  $y$
- corresponding reference values  $s_{ref}^B$

and provides two alternative outputs, each containing all calibration information:

- calibration parameters  $\theta$
- calibration matrix  $C$

Equation (2.3) can be restated to get the measurement in body frame coordinates as a function of the sensor output:

$$s^B = h(y, \theta) = TK^{-1}(y - b) \quad (2.5)$$

where  $\theta$  is the parameter vector defined in equation (2.3).

Alternatively, the parameters can be stored in a homogeneous calibration matrix  $C$ . This format is more compact than the separate parameters in  $\theta$  and it is very useful for applications, as only one matrix multiplication is needed to get calibrated values from raw sensor output values:

$$s^B = C \cdot y_{hom} \quad (2.6)$$

where  $y_{hom}$  is the sensor output in homogeneous coordinates and  $C$  is the 3-by-4 calibration matrix defined as

$$C = [TK^{-1} \quad -TK^{-1} \cdot b]. \quad (2.7)$$

Since the sensor error model is linear, the obvious choice to solve this problem is a linear least squares approach. It requires an equation of the form

$$f(y_i, \beta) = \sum_{j=1}^m \beta_j \phi_j(y_i) \quad (2.8)$$

where the coefficients  $\phi_j$  are functions of  $y_i$ .

In this case the coefficients are

$$\begin{aligned} \phi_1(y) &= \begin{bmatrix} y_x \\ 0 \\ 0 \end{bmatrix}, \quad \phi_2(y) = \begin{bmatrix} y_y \\ 0 \\ 0 \end{bmatrix}, \quad \phi_3(y) = \begin{bmatrix} y_z \\ 0 \\ 0 \end{bmatrix}, \quad \phi_4(y) = \begin{bmatrix} 1 \\ 0 \\ 0 \end{bmatrix}, \\ \phi_5(y) &= \begin{bmatrix} 0 \\ y_x \\ 0 \end{bmatrix}, \quad \phi_6(y) = \begin{bmatrix} 0 \\ y_y \\ 0 \end{bmatrix}, \quad \phi_7(y) = \begin{bmatrix} 0 \\ y_z \\ 0 \end{bmatrix}, \quad \phi_8(y) = \begin{bmatrix} 0 \\ 1 \\ 0 \end{bmatrix}, \\ \phi_9(y) &= \begin{bmatrix} 0 \\ 0 \\ y_x \end{bmatrix}, \quad \phi_{10}(y) = \begin{bmatrix} 0 \\ 0 \\ y_y \end{bmatrix}, \quad \phi_{11}(y) = \begin{bmatrix} 0 \\ 0 \\ y_z \end{bmatrix}, \quad \phi_{12}(y) = \begin{bmatrix} 0 \\ 0 \\ 1 \end{bmatrix} \end{aligned} \quad (2.9)$$

where  $y_j$  is the  $j$ -th component of the measurement vector  $y$ .

Using  $Y_{ij} = \phi_j(y_i)$  and equation (2.9) we get

$$Y_i = \begin{bmatrix} y_{i,x} & y_{i,y} & y_{i,z} & 1 & 0 & 0 & 0 & 0 & 0 & 0 & 0 & 0 \\ 0 & 0 & 0 & 0 & y_{i,x} & y_{i,y} & y_{i,z} & 1 & 0 & 0 & 0 & 0 \\ 0 & 0 & 0 & 0 & 0 & 0 & 0 & 0 & y_{i,x} & y_{i,y} & y_{i,z} & 1 \end{bmatrix} \quad (2.10)$$

where  $y_{i,j}$  is the  $j$ -th component of the  $i$ -th measurement vector  $y_i$ .

$Y$  is a  $(3i)$ -by-12 matrix.

The intermediate parameter vector  $\beta$  is obtained using linear least squares. Thus

$$\beta = (Y^T Y)^{-1} Y^T s_{ref}^B \quad (2.11)$$

where  $s_{ref}^B$  is the reference value of the measured quantity.

From  $\beta$ , the calibration matrix  $C$  can be calculated as

$$C = \begin{bmatrix} \beta_1 & \beta_2 & \beta_3 & \beta_4 \\ \beta_5 & \beta_6 & \beta_7 & \beta_8 \\ \beta_9 & \beta_{10} & \beta_{11} & \beta_{12} \end{bmatrix}. \quad (2.12)$$

This calibration matrix usually suffices as an output. Nevertheless, if needed, the actual parameters of the sensor error model can be calculated: The components of  $\beta$  as a function of the components of  $\theta$  are

$$\begin{aligned} \beta_1 &= \frac{1}{k_x}, \quad \beta_2 = -\frac{\alpha_{yz}}{k_y}, \quad \beta_3 = \frac{\alpha_{zy}}{k_z}, \quad \beta_4 = -\frac{1}{k_x}b_x + \frac{\alpha_{yz}}{k_y}b_y - \frac{\alpha_{zy}}{k_z}b_z \\ \beta_5 &= \frac{\alpha_{xz}}{k_x}, \quad \beta_6 = \frac{1}{k_y}, \quad \beta_7 = -\frac{\alpha_{zx}}{k_z}, \quad \beta_8 = -\frac{\alpha_{xz}}{k_x}b_x - \frac{1}{k_y}b_y + \frac{\alpha_{zx}}{k_z}b_z \\ \beta_9 &= -\frac{\alpha_{xy}}{k_x}, \quad \beta_{10} = \frac{\alpha_{yx}}{k_y}, \quad \beta_{11} = \frac{1}{k_z}, \quad \beta_{12} = \frac{\alpha_{xy}}{k_x}b_x - \frac{\alpha_{yx}}{k_y}b_y - \frac{1}{k_z}b_z. \end{aligned} \quad (2.13)$$

Thus, the desired parameters  $\theta$  can be calculated from  $\beta$  as

$$\begin{aligned} k_x &= \frac{1}{\beta_1}, & k_y &= \frac{1}{\beta_6}, & k_z &= \frac{1}{\beta_{11}}, \\ \alpha_{yz} &= -\frac{\beta_2}{\beta_6}, & \alpha_{zy} &= \frac{\beta_3}{\beta_{11}}, & \alpha_{xz} &= \frac{\beta_5}{\beta_1}, \\ \alpha_{zx} &= -\frac{\beta_7}{\beta_{11}}, & -\alpha_{xy} &= \frac{\beta_9}{\beta_1}, & \alpha_{yx} &= \frac{\beta_{10}}{\beta_6} \end{aligned} \quad (2.14)$$

and

$$\begin{bmatrix} b_x \\ b_y \\ b_z \end{bmatrix} = - \begin{bmatrix} \beta_1 & \beta_2 & \beta_3 \\ \beta_5 & \beta_6 & \beta_7 \\ \beta_9 & \beta_{10} & \beta_{11} \end{bmatrix}^{-1} \begin{bmatrix} \beta_4 \\ \beta_8 \\ \beta_{12} \end{bmatrix} \quad (2.15)$$

## 2.4 Rotation Schedule

The reference orientations and rotations are chosen to excite each axis and cross-sensitivity in at least one configuration, i.e. reflect the effect of all parameters to be calibrated [7]. Each IMU input axis is placed upward, sideways and downward and in every possible orientation halfway in between. See figure 2.2.

Several rotational speeds are sampled for the gyros, from standstill to the maximum measurable value.

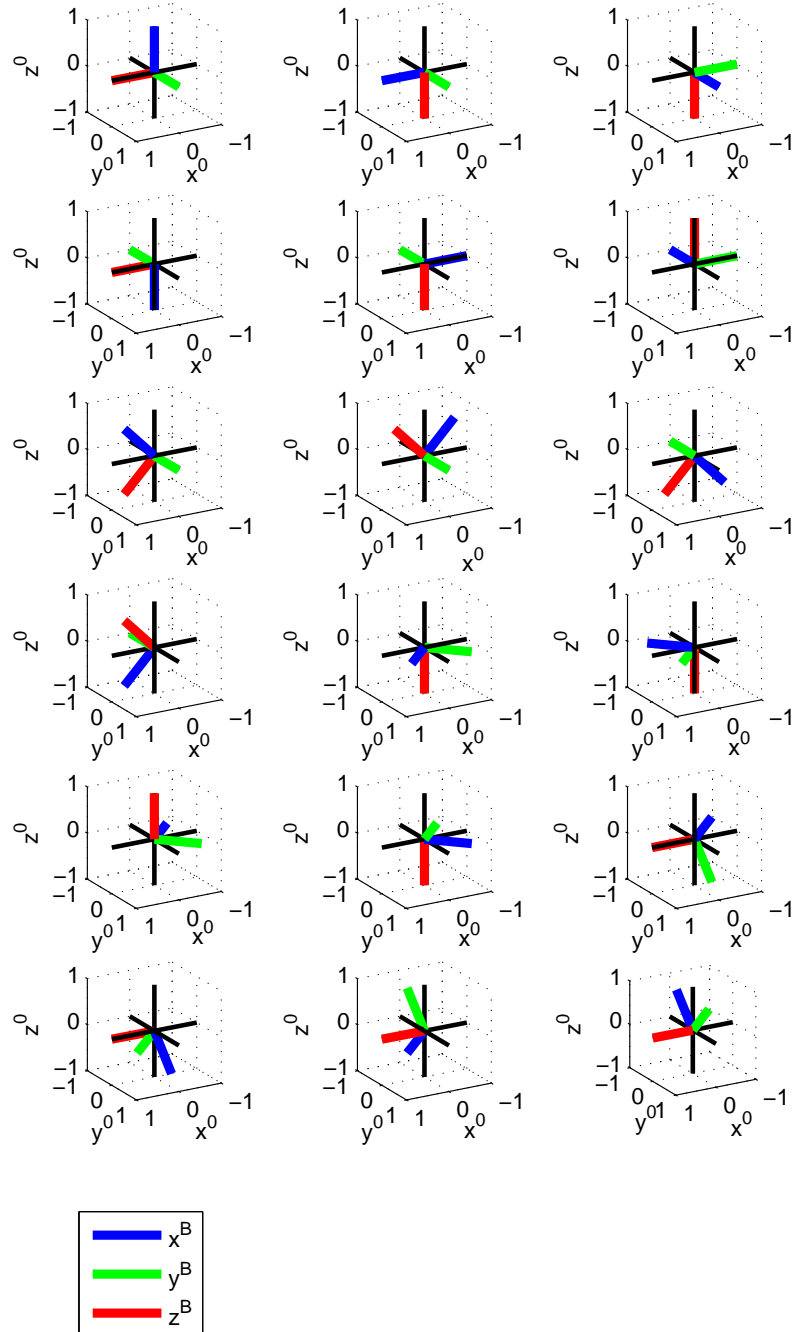


Figure 2.2: Rotation schedule. The IMU body frame  $x$ -axis is coloured red, the  $y$ -axis green and the  $z$ -axis blue. The coordinate frame in each individual image represents the inertial frame.



# Chapter 3

## Mechanical Design

### 3.1 Overview

The mechanical platform is designed as a three DoF gimbal system. It is by far the most commonly used concept. It is straight-forward to implement, especially compared to more complex setups such as the carpal wrist.

Each axis of the system is actuated (see section 3.5). No additional linear actuators are used to generate accelerations higher than 1g: an additional linear actuator would greatly increase the system's complexity and does not justify the presumed slightly better calibration performance.

The system consists of a base and three gimbals. Design details are discussed in the following sections.

A CAD model of the calibration system with indicated axes is depicted in figure 3.1.

### 3.2 Gimbals

There are three gimbals: the *outer*, *middle* and *inner gimbal*, see figure 3.2. All gimbals are made out of aluminium.

The middle and inner gimbal are used to precisely position the IMU, i.e. select the IMU input axis, and the outer gimbal is used for the constant rotation needed for the gyroscope calibration. Thus, this constant rotation is always around the inertial frame z-axis. Consequently, this axis has to be manually aligned to the gravity vector.

The middle and inner gimbal are used to precisely position the IMU, i.e. select the IMU input axis, and the outer gimbal is used to generate the constant rotation needed for the gyroscope calibration.

For the accelerometer calibration, the selected IMU input axis is aligned to the gravity vector and gravity is measured. For the gyro calibration, the selected axis is aligned to the rotation axis of the outer gimbal and its constant rotational speed is measured. In order to use the same alignments – and thus the same rotation schedule – for the calibration of both sensor types, the rotation axis of the outer gimbal has to be manually aligned to the gravity vector. This is done using the adjusting screws on the base and a two-axis water level that is attached to the outer gimbal.

Another two-axis water level is mounted on the inner gimbal. It is used to determine the zero positions of the middle and inner gimbal.

An adapter plate ensures a quick and simple installation and removal of the IMU. Furthermore, if the system were to be adapted for a different IMU, the adapter

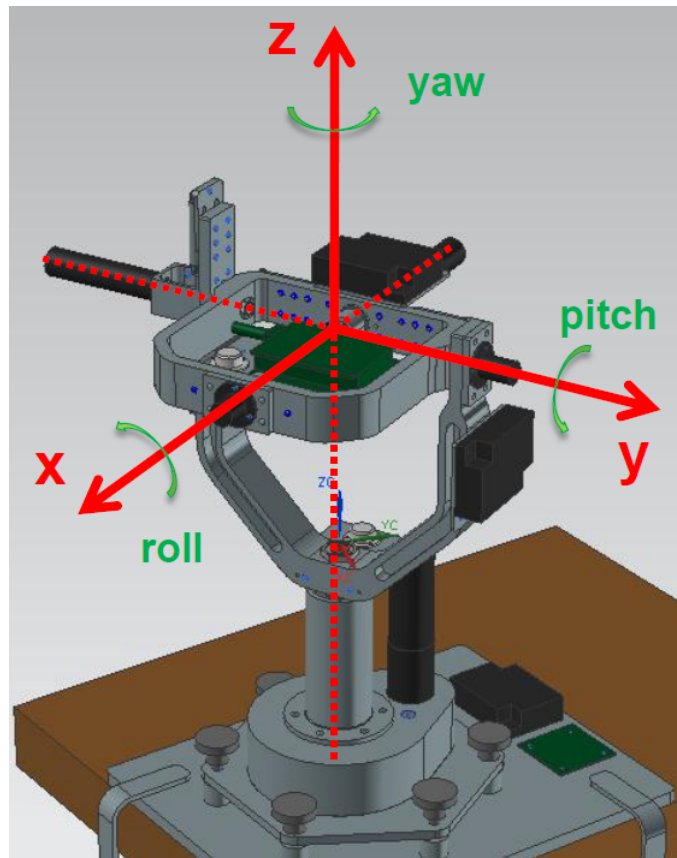


Figure 3.1: Rotation axes of the calibration system.

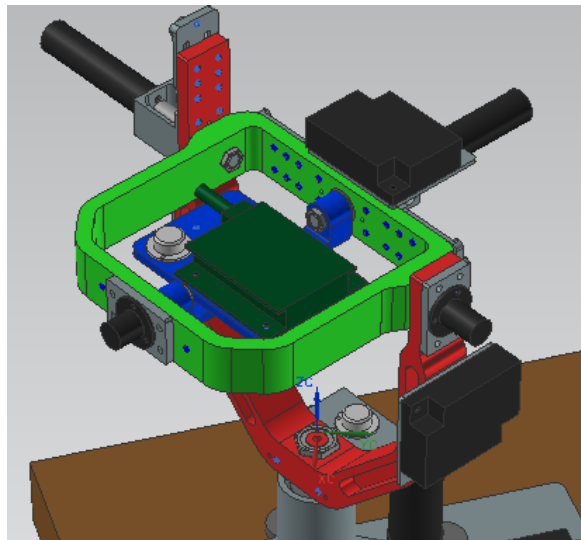


Figure 3.2: gimbals of the calibration system. The outer gimbal is shown in red, the middle gimbal in green and the inner gimbal with the mounting plate in blue. The IMU in dark green is attached to the mounting plate.

plate would be the only mechanical part requiring redesign.

### 3.3 Shafts

#### 3.3.1 Shaft Design

All shafts are made out of steel. There are three shafts implemented in the system: The *outer shaft* is hollow and consists of one part, the *middle* and *inner shaft* that are identical each consist of two parts: A hollow one on the respective slip ring side of the gimbal and a solid one on the motor side. See figures 3.3 and 3.4.

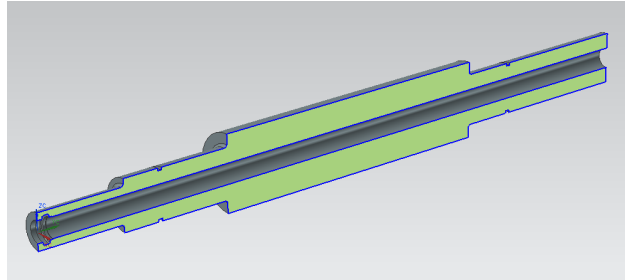


Figure 3.3: Section view of the outer shaft.

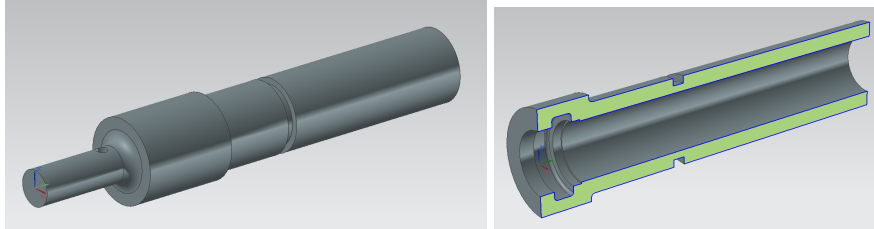


Figure 3.4: The two parts of the middle and inner Shaft. Left: motor side part, right: section view of the slip ring side part

The key feature of the outer shaft and the middle and inner shaft parts on the slip ring sides is their centre hole. It is required to guide the wires from the slip rings through the shaft.

The middle and outer shafts' motor side parts each feature a small through hole in radial direction located near the couplings. They act as an attachment point for the strings leading to the backlash-preventing springs (see section 3.5.3).

#### 3.3.2 Ball Bearings

Sealed ball bearings were implemented for all joints. Ball bearings are widely used due to their overall good performance. While mainly thought for supporting radial forces, they can also accommodate for small axial forces. For each shaft, one fixed and floating bearing are used. The fixed bearing of the outer shaft is a double row angular contact ball bearing, to support the axial force resulting from the weight of the gimbals. Contrary to regular ball bearings, angular contact ball bearings are specifically designed to withstand both radial and axial forces [11]. A double row bearing was chosen to account for axial forces in both directions, in the case of turning over the whole system, for example during transport. Note that the ball bearings of the middle and inner shaft are also subject to axial forces depending

on the orientation and rotational speed of the platform. However, these forces are rather small and can easily be handled by the standard ball bearings. Sealed bearings were chosen to ensure a lifelong lubrication, reducing the required maintenance of the system.

### 3.3.3 Slip Rings

At each joint, slip rings were implemented to be able to freely rotate the system around each axis for an unlimited number of rotations. These state-of-the-art slip rings can handle up to two amperes per ring and are suited for transmitting digital and analogue signals. While unlimited rotation for the gimbals is not a necessity, it simplifies the calibration and provides a cleaner and more appealing design solution. Especially for the gyroscope calibration, it is preferable to be able to rotate the outer gimbal indefinitely. Note that the middle and inner gimbal's rotation is limited nonetheless due to attached springs preventing backlash (see section 3.5.3).

## 3.4 Base

The base consists of two parts: a fixed plate that is clamped to a table and an adjustable part that holds the motor and the outer shaft with its bearings. The latter part is adjustable relative to the former by manually manipulating three screws. Another three screws are used to fasten the adjustable part to the plate. The adjusting is needed to align the axis of the outer shaft to the gravity vector.

A section view of the upper part of base is depicted in figure 3.5, the base plate is shown in figure 3.6.

All milled and turned parts of the base are made out of aluminium, except for the steel shaft.

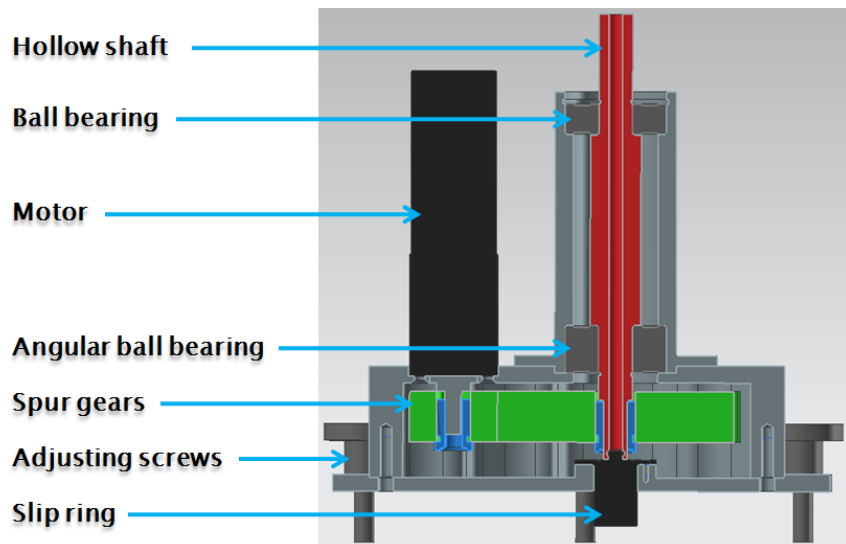


Figure 3.5: Section view of the upper part of the base.

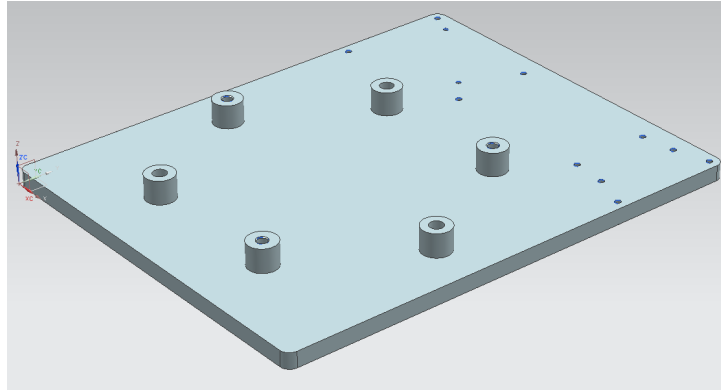


Figure 3.6: Base plate. It is clamped onto a table.

## 3.5 Actuation

### 3.5.1 Motor Specifications

All implemented motors, gear heads and controllers are Maxon products. For the middle and inner shaft, 4.5W RE16 motors were chosen and for the outer shaft, a 20W RE25 motor. All motors need a 24V DC power supply.

### 3.5.2 Couplings

To prevent blocking the system due to manufacturing and assembly inaccuracies and shaft expansion, couplings were used on the middle and inner gimbals' motor shafts. in the outer gimbal, the shaft is relieved by a set of spur gears. Furthermore, the spur gears are mechanically necessary in order to be able to attach a slip ring to the outer shaft.

### 3.5.3 Backlash Prevention

Since the middle and inner gimbal have to be positioned precisely, the backlash has to be kept to a minimum. Therefore the play introduced by the gear heads of the motors powering the middle and inner gimbal has to be eliminated. This is achieved by applying a continuous torque to the gear head shafts using two springs pulling on opposing sides of the shaft circumference. Unfortunately, this fact mechanically limits the number of possible rotations for the affected gimbals, as the spring cannot extend indefinitely. Additionally, the applied torque is not constant due to the springs' extension. Each motor still has to be able to move the corresponding gimbal at the maximum torque position, but at the same time, the minimum torque has to be strong enough to hold all stages of the gear heads in place. See figure 3.7 for an illustration.

The springs are attached to the shafts by a spectra kite string.  
Note that in reality there's still a very small residual backlash.

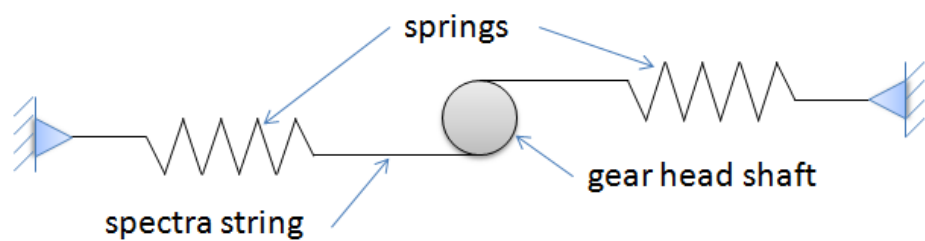


Figure 3.7: Backlash prevention. The two springs are attached to opposing sides of the gear head shaft, generating a pure torque without any radial forces.

# Chapter 4

## Electronics

An overview over the electronic components is given in this chapter, including the wiring with its slip rings, the used motor controllers and the interface PCB. For a more in-depth description of these elements, please refer to the calibration system manual in appendix A.

### 4.1 Wiring

As stated in section 3.3.3, slip rings were implemented at each axis. For most of the wiring on the gimbals, the inherent cables of these slip rings were used. The only exception being the ribbon cable between each motor and its controller. To limit interference, corresponding pairs of strands for data and power have been intertwined with each other and contact rings next to each other were used in the slip rings. A simplified wiring diagram is depicted in figure 4.1.

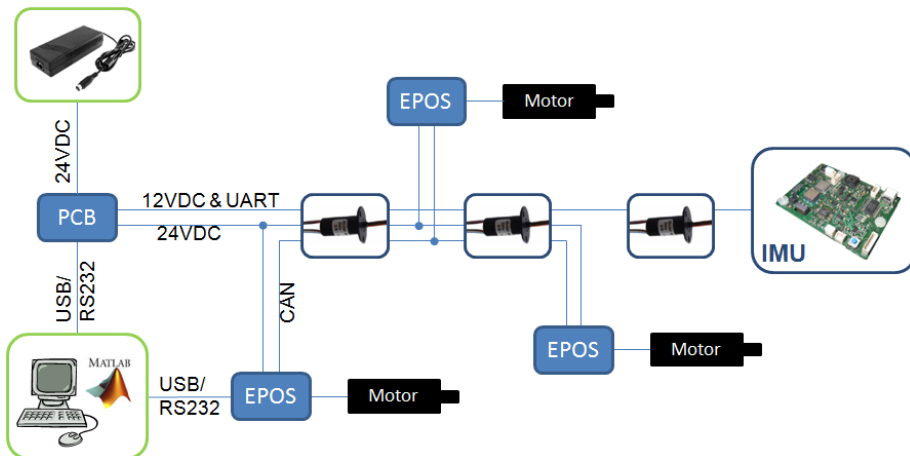


Figure 4.1: Simplified wiring diagram of the calibration system. The PCB was specifically designed for this system, see section 4.3.

### 4.2 Motor Controller

For each motor, a Maxon EPOS 24/2 controller was used. They provide position and velocity control for the motors. The motor controller of the outer gimbal is

directly connected to a computer via USB or RS232. The other two controllers are linked by a CAN network.

### 4.3 PCB

The calibrations system's PCB simplifies the connections and provides circuit protection. It has got a mini-USB and a COM-port socket for the IMU communication. The interface can be selected using an onboard switch. Figure 4.2 shows an overview of the PCB.

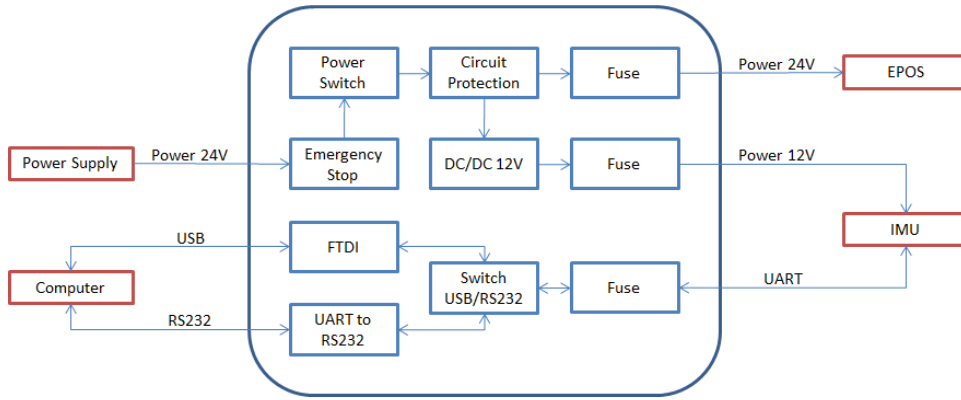


Figure 4.2: Overview of the calibration system's PCB.

The PCB also features a DC/DC converter to provide the 12V power for the IMU. Thus, the whole system only needs 24V DC power supply. It has built-in protection against reverse polarity, overvoltage and ESD.

Because the slip rings are easily destroyed by high currents, all strands leading through slip rings are fused, including the data lines.

Detailed schemes of the PCB can be found in section A.6.5 of the calibration system manual.

# **Chapter 5**

## **Software**

Motor control via Matlab, the communication with the IMU and key features of the implemented GUI are discussed in this chapter. More detailed information, in particular regarding the GUI, can be found in the calibration system manual in appendix A.

### **5.1 Motor Control**

The control of the motors was achieved using a Windows library provided by Maxon. With a few tweaks to the library header file – mainly variable type definitions – it was possible to load it into Matlab. This allows direct control of the motors through Matlab code.

Matlab equivalents of many functions of the mentioned library were written. The whole software suite is provided on the DVD attached to this report.

### **5.2 IMU Communication**

The communication with the IMU is simple: the IMU is programmed to continuously send 12-bit ADC output values in the format of ASCII characters over UART. This data can be read by the calibration system any time it is needed. Communication is unidirectional, the calibration system only listens and reads sensor values. Note that the rate at which the IMU sends the data does not matter, it will just affect the calibration time.

### **5.3 GUI**

A simple Graphical User Interface (GUI) for the IMU calibration was implemented in Matlab. It features simple setup of the connections, easy adjustment of the calibration parameters and user accounts with storable settings. The actual calibration can be done by pressing a single button, without any necessary further interactions. There's also an integrated GUI for defining the zero positions of the gimbals. Screenshots of the main GUI and the zero position GUI can be found in figures 5.1 and 5.2, respectively.

The algorithm described in section 2.3 was incorporated into the GUI.  
The implemented Matlab functions are listed in table 5.1

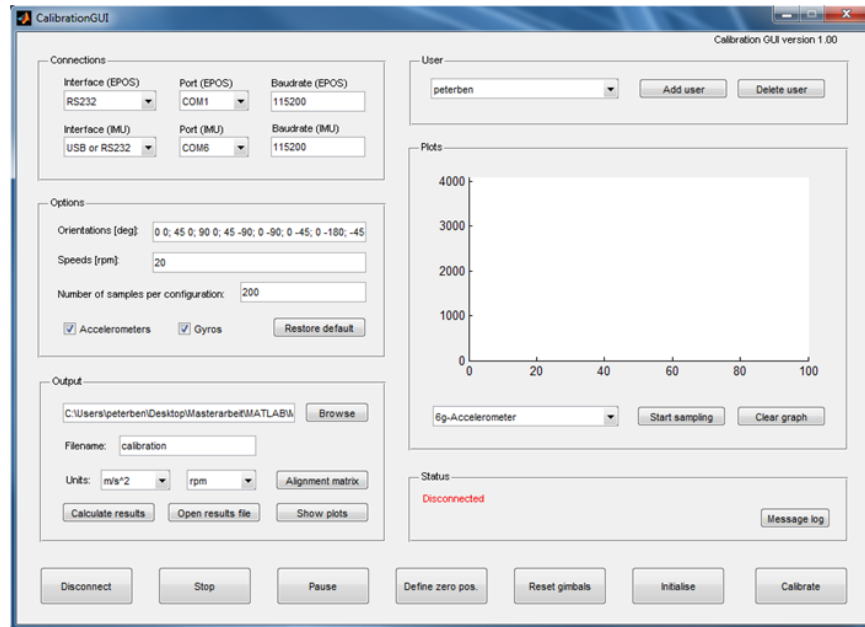


Figure 5.1: Screenshot of the Calibration GUI

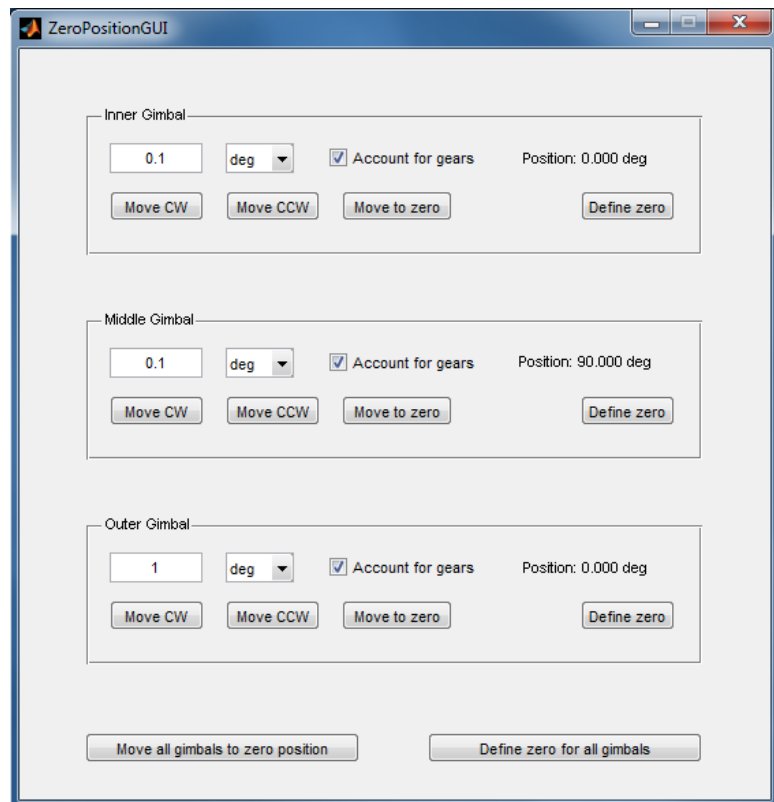


Figure 5.2: Screenshot of the GUI for defining the zero positions of the gimbals.

Table 5.1: List of Matlab functions

Main functions	
CalibrationGUI	Main file of the Calibration GUI
ZeroPositionGUI	Main file of the GUI for defining the zero positions of the gimbals
InitialiseEPOS	Custom EPOS initialisation
calibration_algorithm	Implementation of the calibration algorithm
calculate_reference_values	Calculate reference values from rotation schedule

Results and visualisation functions	
plot_calibration	Plot calibrated data and reference values
validation	Validate calibration data and compare it to nominal values
repeatability	Calculate maximum change of each parameter type over a set of calibrations
repeatability_plots	Compare scale values of several calibrations
rotation_schedule	Visualisation of the rotation schedule

Auxiliary functions	
shift_samples	Shift samples by a bias vector
rot	Calculate a specific rotation matrix
mat2theta	Convert a calibration matrix into sensor error model parameters
theta2mat	Convert sensor error model parameters into a calibration matrix



# Chapter 6

# Calibration Procedure and Test Results

## 6.1 Calibration Procedure

Before a calibration can be done, the system has to be set up, including

- Connecting external wires
- Installing the correct firmware on the IMU
- Mounting the IMU on the inner gimbal
- Adjusting the base of the system to the gravity vector
- Setting the connection options in the GUI

An actual calibration consists of the following steps:

- Defining the zero positions of the gimbals
- Setting the calibration and output options
- Start sampling

A more detailed description of the calibration procedure can be found in the manual in section A.4.

## 6.2 Results

The result of the test calibrations produced reasonable output values within the expected ranges.

As an example, the calibration matrix of the 6g-accelerometer is shown in figure 6.1. Recall: The sensor ADC output values in homogeneous coordinates is multiplied by this calibration matrix to get the desired physical quantity – linear acceleration in this case – in IMU body frame coordinates.

An interesting observation is that the scale values of the sensors differ between each axis by amounts of up to the order of percent. This applies to both sensor types, accelerometers and gyros. The cross sensitivities are in the order of up to a few percent of the scale values.

<b>0.03248</b>	-0.00067	0.00022	<b>-71.482</b>
-0.00041	<b>0.03301</b>	-0.00032	<b>-72.696</b>
-0.00010	0.00034	<b>0.03256</b>	<b>-73.407</b>

Figure 6.1: Example of a calibration matrix (6g-accelerometer). The scale values are marked red, the biases green and the cross sensitivities grey.

### 6.3 Validation

The calibration matrices were validated on different data sets. The calibrated values were compared to the nominal values calculated according to the sensor data sheets. The validation and comparison for the different sensors is shown in figures 6.2 through 6.4. Close-ups of selected sections of these graphs can be found in figures 6.5 and 6.6.

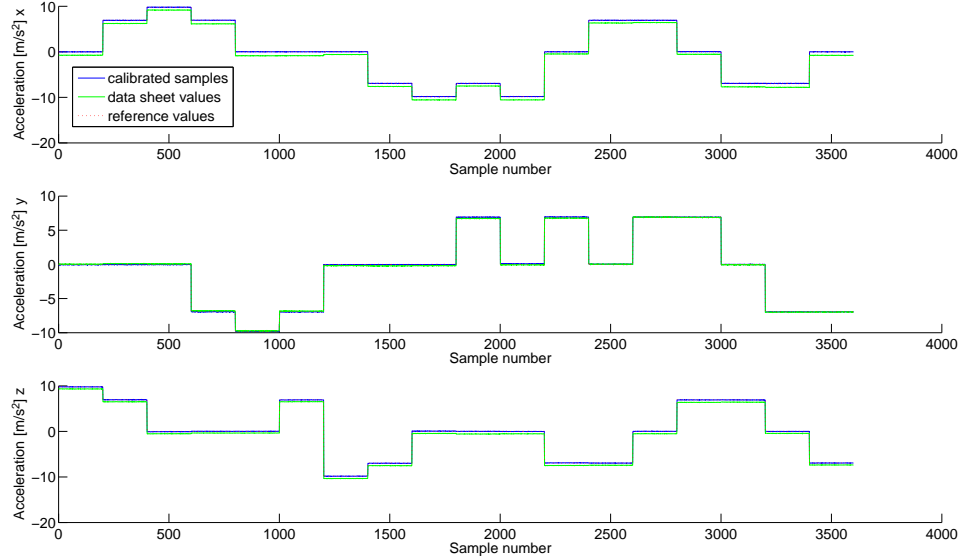


Figure 6.2: Comparison of calibrated values to expected values according to the sensor data sheet of the 6g-accelerometer.

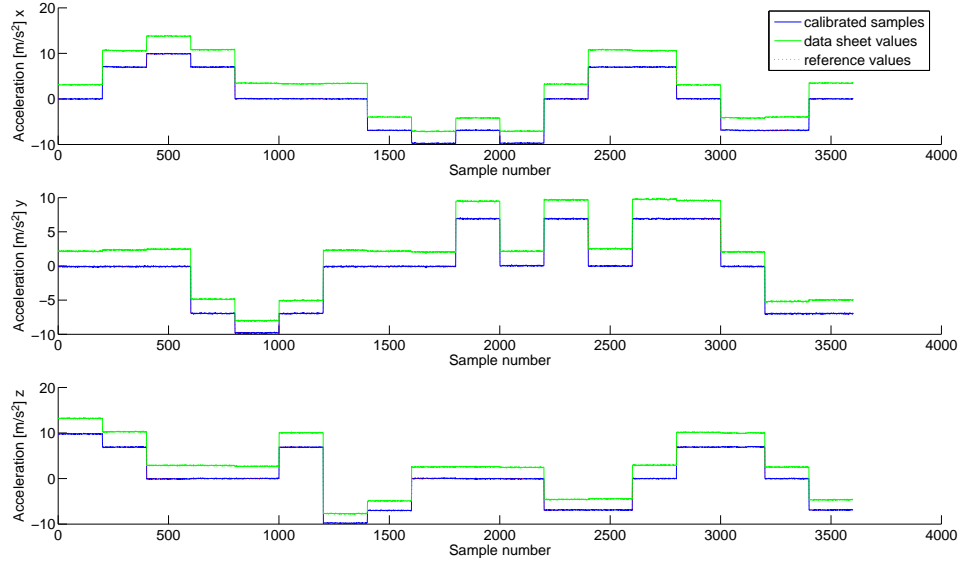


Figure 6.3: Comparison of calibrated values to expected values according to the sensor data sheet of the 1.5g-accelerometer.

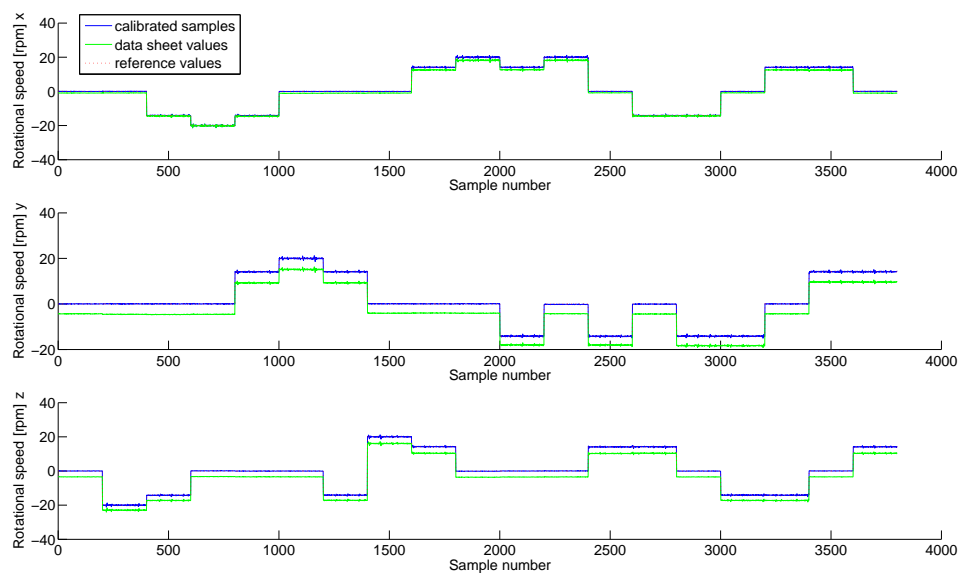


Figure 6.4: Comparison of calibrated values to expected values according to the sensor data sheet of the gyro. The reference value is the set point of the motor velocity controller, the controller is assumed to be significantly more accurate than the gyro measurement.

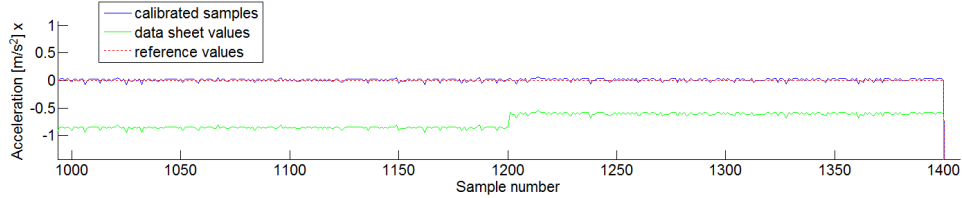


Figure 6.5: Closeup of figure 6.2.

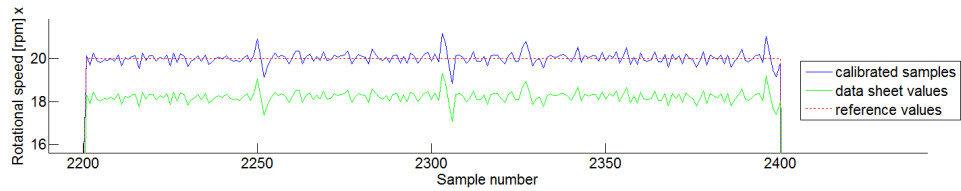


Figure 6.6: Closeup of figure 6.4.

Notice in figure 6.5 that the cross-sensitivities, clearly visible in the data sheet values, are no longer there after the calibration.

## 6.4 Accuracy of the Calibration System

The accuracy of the calibration system itself is mostly linked to the accuracy of the positioning of the middle and inner gimbal and the initial alignment of the outer gimbal axis. The nominal sensitivity of the water levels is 20', which is rather conservative. Because the adjustments are done using motors and adjusting screws, respectively, the actual sensitivity is better. An accuracy of about one tenth of a degree can be achieved.

The accuracy of the generated rotational speeds is not perfect due to small oscillations induced by the spur gears and the system itself. However these effects will be significantly reduced and eventually cancelled out if the gyro is sampled long enough.

The manufacturing and assembly precision of the system was measured using equipment with sensitivities of 30" for angles and 10µm for lengths. It proved to be orders of magnitudes better than the accuracy achieved by the manual positioning.

## 6.5 Repeatability

Multiple calibrations were done over the course of several days. The system was relocated and readjusted several times in between. As examples, the x-axis scale values of the two accelerometers are shown in figure 6.7

According to the mentioned calibrations, some observations on the magnitude of change of the different parameter types between calibrations can be made. They are listed in table 6.1. This table is intended to give a rough estimation on how long a calibration is valid. The values are of course affected by sensor drifts, particularly visible on the 1.5g-accelerometer.

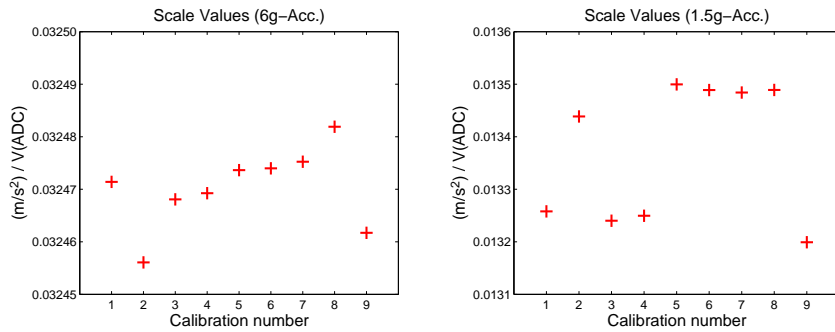


Figure 6.7: Repeatability: x-axis scale values of the two accelerometers from different calibrations.

Table 6.1: Changes of the different parameter types between calibrations.

Parameter	6g-Acc.	1.5g-Acc.	Gyro
Scale	< 0.2%	< 5%	< 0.2%
Cross sensitivity (relative to scale)	< 0.5%	< 0.05%	< 0.05%
Bias	< 0.5%	< 5%	< 0.5%



# Chapter 7

## Conclusion

A three degrees of freedom gimbal system has been designed and built. It is capable of calibrating the ASL IMU without the need for manual repositioning. The calibration is controlled from a GUI. A manual was written for the calibration system. The whole system can easily be extended with additional features or adapted to other IMUs or sensors. Especially the software, including the GUI, can be adjusted on the fly to ones needs, since its written in Matlab.

The obtained calibration parameters correspond to the expected ranges from the data sheets. Considering different scale values for each sensitivity axis and cross sensitivities instead of using just one scale value for every sensitivity axis and no cross sensitivities resulted in a significantly more accurate calibration.

A calibration proved to be valid over an extended period of time, except for the 1.5g accelerometer, which exhibits a rather large drift.

The calibration of the ASL IMU now takes a lot less time and effort.

An improvement to the system would be to store the calibration data directly onto the IMU. Additionally, it would be desirable to be able to give a precise estimation of the accuracy of the calibration matrix. Assessing the performance of the calibration data on actual systems would also provide interesting insights.



## Appendix A

# Calibration System Manual

### A.1 Introduction

This manual on the calibration system for the ASL IMU contains technical information and a guide to set up the system and perform a calibration.

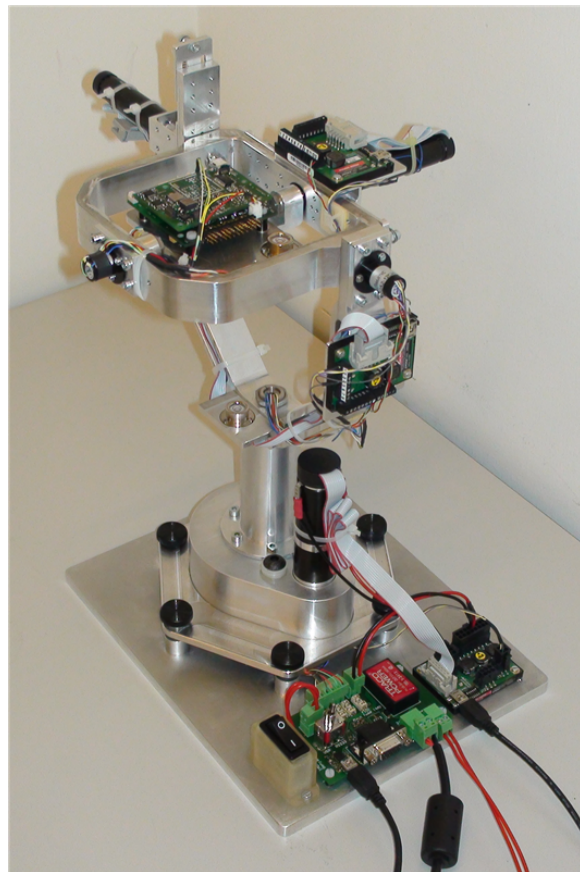


Figure A.1: The Calibration System.

## A.2 Calibration System Overview

The calibration system has three independently actuated gimbals and thus three degrees of freedom (DoF). The axes of the system are marked in figure A.2.

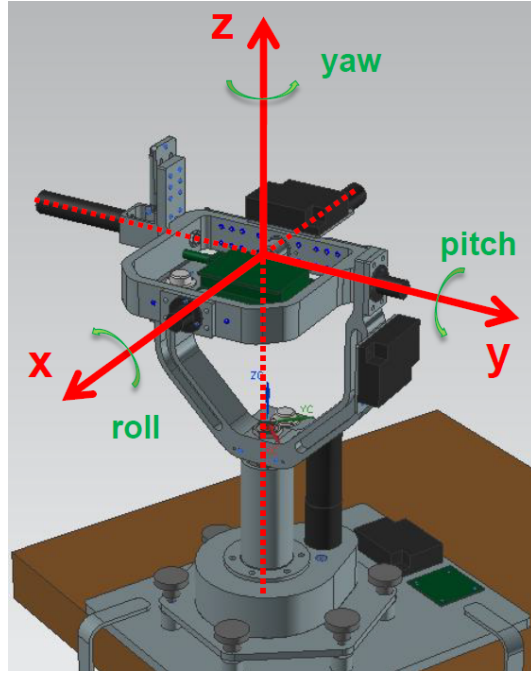


Figure A.2: Axes of the calibration system.

There is an *outer*, a *middle* and an *inner gimbal*. The middle and inner gimbal are used to precisely position the IMU, i.e. select the IMU input axis, and the outer gimbal is used for the constant rotation needed for the gyroscope calibration. Thus, this constant rotation is always around the inertial frame z-axis. Consequently, this axis has to be manually aligned to the gravity vector.

The middle and inner gimbal are used to precisely position the IMU, i.e. select the IMU input axis, and the outer gimbal is used to generate the constant rotation needed for the gyroscope calibration.

For the accelerometer calibration, the selected IMU input axis is aligned to the gravity vector and gravity is measured. For the gyro calibration, the selected axis is aligned to the rotation axis of the outer gimbal and its constant rotational speed is measured. In order to use the same alignments – and thus the same rotation schedule – for the calibration of both sensor types, the rotation axis of the outer gimbal has to be manually aligned to the gravity vector. This is done using the adjusting screws on the base and a two-axis water level that is attached to the outer gimbal.

Another two-axis water level is mounted on the inner gimbal. It is used to determine the zero positions of the middle and inner gimbal.

## A.3 Setup

### A.3.1 Required External Wiring

The minimal external wiring consists of the following cables:

- 24V DC Power Supply
- USB A-mini-B cable or standard RS232 serial cable (DB-9) for the IMU communication
- USB A-mini-B cable or Maxon EPOS specific RS232-COM cable for the motor controllers

If the emergency stop or the power switch is not used, the two pins of the corresponding header have to be connected. Otherwise, the system cannot be powered.

### A.3.2 IMU Firmware

The IMU has to be set up to continuously send ADC sensor output values as ASCII characters over UART. The current ASL IMU contains two accelerometers (ST Microelectronics LIS344ALH and Memsic MXR9500) with a range of  $\pm 6g$  and  $\pm 1.5g$ , respectively, and one gyro (Analog Devices ADXRS610), each with three axes. Thus, one line of sent data consists of nine values. The order of these values is defined in table A.1.

Table A.1: Order of values of the data vector sent by the IMU.

Number	Content
1	6g-Accelerometer x-axis
2	6g-Accelerometer y-axis
3	6g-Accelerometer z-axis
4	1.5g-Accelerometer x-axis
5	1.5g-Accelerometer y-axis
6	1.5g-Accelerometer z-axis
7	Gyro x-axis
8	Gyro y-axis
9	Gyro z-axis

The frequency at which the data is sent does not have an impact on the calibration itself, but does affect the duration of the calibration.

### A.3.3 IMU Mounting

The motherboard of the ASL IMU has to be screwed onto the mounting plate, which is then attached to the inner gimbal. To calibrate a different IMU, it can simply be exchanged. There is no need to detach the motherboard.

The motherboard has to be connected to the calibration system according to the scheme found in section A.6.4.

If the IMU body frame axes do not coincide with the calibration system body frame axes shown in figure A.2, an alignment matrix has to be defined. This matrix transforms IMU body frame coordinates to calibration system body frame coordinates, i.e.

$$A = T_{b,IMU}^{b,CalibSys}. \quad (\text{A.1})$$

The alignment matrix is typically a permutation matrix that can easily be determined. The default is the identity matrix. It can be changed by pressing the 'Alignment matrix' button in the output panel of the GUI.

### A.3.4 Setting up Connections

As mentioned in section A.3.1, the communication with the IMU and the motor controllers each can be done via USB or RS232. For the communication with the IMU, the data switch (S100) on the calibration system's board has to be set to USB or RS232, according to the used cable. Note that in version 1.0 of the board, the labels of the switch are inverted by mistake. A driver has to be installed from the EPOS CD, in order for the motor controllers to be recognised.

For the next steps, the calibration GUI must be started by executing the 'CalibrationGUI.m' file. For the IMU communication, the proper COM port has to be selected in the connections panel of the GUI. It does not depend on which interface was used, as both, USB/FTDI and RS232, are represented by either virtual or physical COM port in Windows. This is different for the motor controller communication, as the EPOS controller is a true USB device recognised as such by Windows, if the driver is installed. Therefore, the interface has to be set first. Then, the right port – USB $n$  or COM $n$  – can be selected.

Another important setting is the baudrate. In the connections panel, it can be set independently for the motor controllers and the IMU communication. For the motor controllers, the default is 115200 baud. This value will never change unless the motor controllers are reprogrammed. On the other hand, the baudrate in the IMU communication input field has to match the baudrate of the IMU output, which depends on the firmware currently installed on the IMU.

To check the IMU communication, press the 'start sampling' button. If the connection works, raw ADC output values will be plotted. If it fails, an IMU read error message will be displayed.

If the connection options were set correctly, but the connection does not work, in most cases unplugging the data cable for a short time or turning the system off and on again solves the problem.

### A.3.5 Initial System Adjustment

To ensure a correct calibration, the vertical axis of the system has to be aligned to the local gravity vector. This is done by adjusting the upper part of the base relative to the base plate. Three of the screws on the base are used to position the upper part and the other three screws are used to fasten it. The fastening screws are marked by a red dot.

Adjusting the system to the gravity vector contains the following steps:

1. Loosen the fastening screws.
2. Adjust the upper part of the base with the help of the water level attached to the outer gimbal by manipulating the adjusting screws.
3. Tighten the fastening screws.

It is best to use screw clamps to hold the base plate in place. Otherwise, the system might have to be readjusted after each calibration, or it might even move during calibration, rendering the output useless.

## A.4 Calibration Procedure

### A.4.1 Preparations

Make sure that the system is properly set up and that the IMU has the right firmware installed.

Start the calibration GUI by executing the 'CalibrationGUI.m' file. Click the 'Initialise' button in the GUI to connect the calibration system and initialise the motor controllers. If the initialisation fails, check whether the wiring and communication are set up correctly.

#### A.4.2 Defining the Zero Positions of the Gimbal

Open the zero position GUI (figure A.3) by pressing the 'Define zero pos.' button. There, the zero position of each individual gimbal can be set. By pressing one of the 'Define zero' buttons, the corresponding gimbal's current position will be defined as its new zero position.

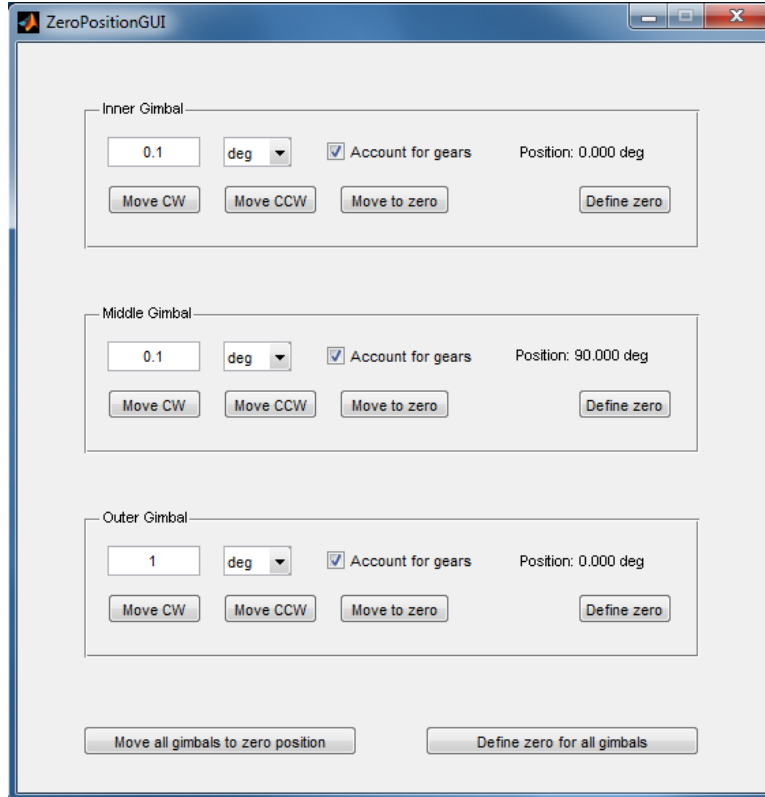


Figure A.3: Separate GUI for defining the gimbals' zero positions.

With the help of the water level attached to the mounting plate, the zero position of the middle and inner gimbal have to be set such that the IMU mounting plate is horizontal. To achieve this, the gimbals are moved by specified angle steps. These angles can be set individually for each gimbal in the top right of its GUI panel. By pressing the button 'Move CW' or 'Move CCW', the corresponding gimbal is rotated relative to its current position by this angle in clockwise or counter-clockwise direction, respectively.

The gimbals can also be moved by the arrow keys. The function of these keys are the same as the corresponding buttons in the GUI, but it is sometimes easier to manipulate the gimbals using the keyboard. The Up and Down arrow keys move the middle gimbal, left and right the inner gimbal. Page up and page down rotates the outer gimbal. The figure of the GUI, not any individual part of it, has to be in focus in order for the keyboard inputs to work.

Note that setting the zero position of the outer gimbal is not crucial, as it has no direct influence on the calibration as long as the base was correctly aligned with gravity.

### A.4.3 Calibration and Output Options

The calibration options can be set in the options panel. The rotation schedule, the rotational speeds for the gyro calibration and the number of samples taken at each configuration can be defined by filling in the corresponding input fields. Additionally, the two check boxes allow to choose which sensor types to calibrate. Detailed information on the calibration options can be found in table A.4.

In the output panel, the folder and filename of the output file can be chosen. The output consists of a text file with all the calibration matrices and a mat-file containing all important Matlab variables. The calibration matrices will also be displayed in the Matlab command window.

Furthermore, the units of the calibration matrices can be set. If the units are changed after the calibration, the calibration matrices have to be recalculated by pressing the 'Calculate results' button, in order for the unit change to take effect. The text output file will be updated as well.

More information on all these options can be found in sections A.5.5 and A.5.6.

## A.5 GUI Features

### A.5.1 Overview

An overview of features of the calibration GUI can be found in figure A.4. These features are explained further in the following sections. Most of them should be self-explanatory.

The library used for the motor controller interface only works on computers using a 32-bit version of Windows.

The GUI is started by executing the 'CalibrationGUI.m' file.

### A.5.2 State and Messages

In the status panel, the current state of the system and potential warning or error messages are displayed. All possible states are listed in table A.2.

Table A.2: States of the calibration GUI

Value	State
-1	Error
0	Disconnected
1	Ready (connected, but not busy)
2	Calibrating (busy)
3	Busy (generic)

If the system is put into the error state by any sub function, all running processes will be stopped. When in error state, most features will not work until the system is reinitialised. The nature of the error is specified by an error message. Warning messages do not indicate a change to the error state, they merely inform about unexpected or unusual incidents.

Warning messages are displayed in orange and error messages in red. Only the newest message is shown in the status panel. A message log can be accessed through

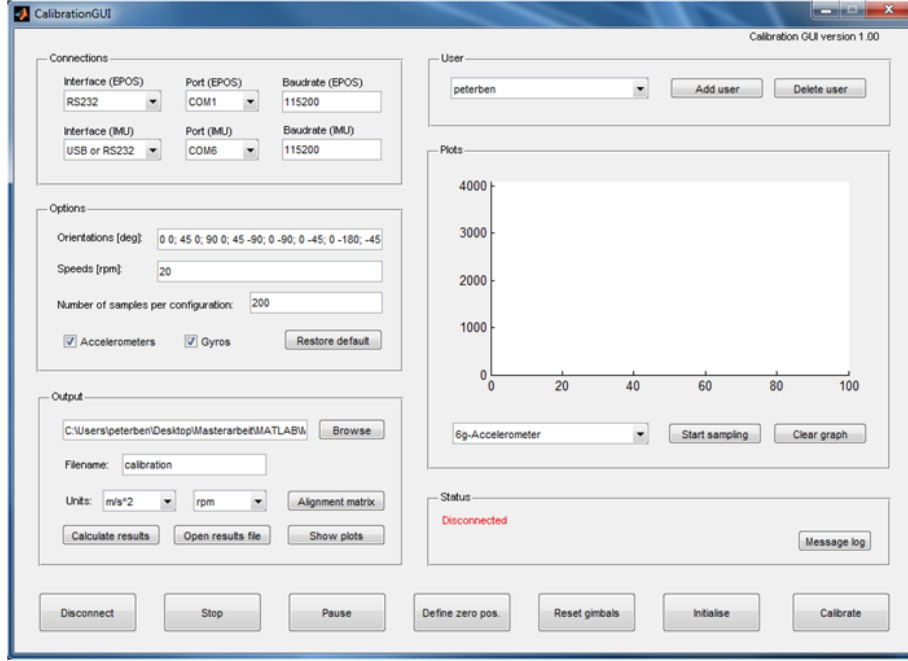


Figure A.4: Features of the GUI. There are panels for calibration options, output options, connection to the IMU and the motor controllers, user selection, system status and plots. On the bottom of the GUI, the main buttons are located.

the 'Message Log' button. It shows all warning and error messages that were displayed since the GUI was started.

### A.5.3 Main Buttons

The functions of the main GUI buttons are described in table A.3.

Table A.3: Main GUI Buttons.

Button	Function
Initialise	Connects the calibration system and initialises motor controllers. It also recovers the system from the error state.
Disconnect	Disconnects the calibration system. This is executed automatically when the GUI is closed.
Calibrate	Starts the calibration. Not possible in error state.
Reset gimbals	Sets all the gimbals to their zero position.
Define zero pos.	Starts a separate GUI to define the zero positions of the gimbals.
Pause	Pauses the running calibration. It does not stop the rotation of the outer gimbal (when calibrating gyros).
Stop	Aborts the calibration. All sensor data from the current calibration is lost.

#### A.5.4 Connections

In the connections panel the used ports for the connection to the motor controllers and to the IMU are selected.

For the IMU communication, only the proper virtual or physical COM port has to be selected.

This is different for the motor controller communication: The interface has to be set first. Then, the right port – USB $n$  or COM $n$  – can be selected.

Furthermore, the baudrates of the motor controller and the IMU communication can be set individually. For the motor controllers, the default is 115200 Bd. This value will never change unless the motor controllers are reprogrammed. The baudrate in the IMU communication input field has to match the baudrate of the IMU output, which depends on the firmware currently installed on the IMU.

#### A.5.5 Options

In the options panel, all possible calibration options can be set. The options are listed in table A.4.

Table A.4: Calibration options.

Option	Function
Orientations	Specifies the rotation schedule of the platform. The first value of every pair of angles corresponds to the pitch angle, the second value to the roll angle.
Speeds	Specifies the speeds at which the gyros are sampled. Multiple values are possible
Number of samples per configuration	Specifies the number of samples that is taken at each configuration
Accelerometers checkbox	If checked, accelerometers are calibrated
Gyros checkbox	If checked, gyros are calibrated
Restore default	Restores default values for all the calibration options.

### A.5.6 Output

In the output panel, the folder and filename of the output file can be chosen. The output is a text file containing the calibration matrices and additional information on the chosen calibration settings. All important Matlab variables, including the raw sensor ADC output values are stored in a mat-file of the same name. If a file with the same name already exists in the specified folder, a number will be automatically added to the filename, starting from '00' to '99'.

Furthermore, the units of the calibration matrices can be set. If the units are changed after the calibration, the calibration matrices have to be recalculated by pressing the 'calculate results' button, in order for the unit change to take effect. The text output file will be updated as well. This also applies, if the alignment matrix (see section A.3.3) was defined wrong: It can be changed later and the results can be recalculated.

Pressing the 'show plots' button displays a plot for each calibrated sensor. These plots show the reference values and the calibrated sensor values for every axis of each sensor.

### A.5.7 Plots

In the plots panel, raw sensor output values can be displayed. It is used to check whether the data sent by the IMU is received and formatted correctly. Note that the sampling frequency is not very high and fluctuating. Thus, when checking the values by manipulating the system manually, keep in mind that sudden movements may not be captured in the graph. To be able to start a calibration, the sampling for the plots panel has to be stopped first, as the samples are needed for the calibration.

### A.5.8 Accounts

In the user panel, the current user account can be selected. All calibration options, the output directory and the output filename are saved individually. Connection information is saved globally for all users. All data is saved automatically whenever it is altered.

The default user and guest user account cannot be deleted. The default user contains all default values in the calibration options and they cannot be changed.

## A.6 Technical Data

### A.6.1 Electrical Data

The electrical data of the calibration system is listed in table A.5.

Table A.5: Electrical Data

Description	Value
Nominal power supply voltage $V_{CC}$	24VDC
Absolute minimum power supply voltage $V_{CC}$	18VDC
Absolute maximum power supply voltage $V_{CC}$	28VDC
Maximum power consumption	<100W
EPOS and motor power supply voltage	24VDC
IMU motherboard power supply voltage	12VDC
Main fuse	4A
Individual power and data strand fuses	2A
Maximum admissible current through slip rings	2A

### A.6.2 Mechanical Data

The mechanical data of the calibration system is listed in table A.6.

Table A.6: Mechanical Data

Description	Value
Maximum rotational speed of outer gimbal	100rpm
Maximum rotational speed of middle and inner gimbal	70rpm
Maximum permissible rotational speed of slip rings	250rpm
Joint limits of middle gimbal	$\pm 90^\circ$
Joint limits of inner gimbal	$\pm 180^\circ$

### A.6.3 Wiring

A simplified wiring diagram of the calibration is shown in figure A.5.

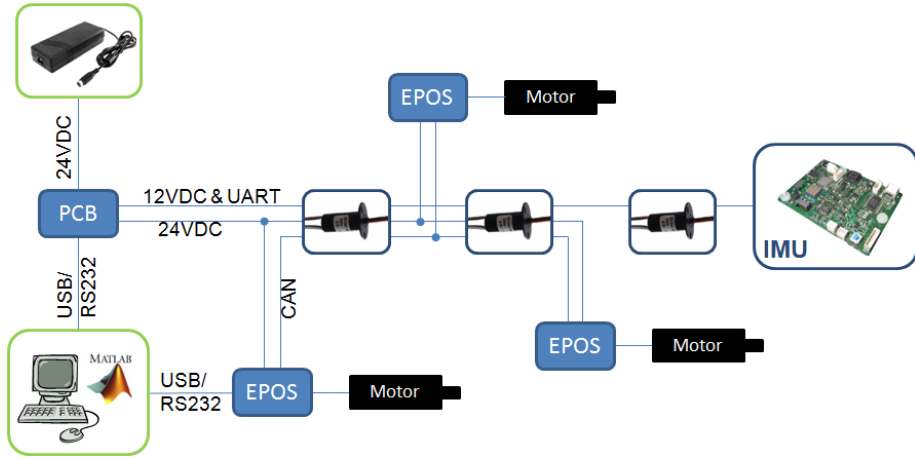


Figure A.5: Simplified wiring diagram of the calibration system.

Table A.7 lists the wiring configuration of the slip ring wires. Their lead size is 28AWG. Note the change in wire insulation colour from the outer and middle slip ring to the inner slip ring due to the fact that adjacent rings were used for each pair of intertwined power and data strands.

Table A.7: Slip ring wire configuration.

Colour	Colour (inner slip ring)	Signal	Description
Red		24VDC	EPOS power supply
Green		GND	EPOS power ground
Yellow		CAN high	CAN high bus line
Purple		CAN low	CAN low bus line
Grey		GND	CAN ground
Dark blue		Not connected	–
Brown	Yellow	GND	IMU power and comm. ground
Orange	Red	12VDC	IMU motherboard power supply
White	White	UART Tx	IMU communication transmit
Khaki	Green	UART Rx	IMU communication receive
Black	Black	Not connected	Broken slip ring
Blue	Blue	Not connected	Broken slip ring

#### A.6.4 Connectors

The pin configuration of connector P101 on the calibration system PCB is listed in table A.8. Information on the connector on the inner gimbal can be found in figure A.6 and table A.9. The pin configurations of all other connectors on the calibration system PCB are straight-forward. More information on the PCB and its connectors is provided in the section A.6.5. For the EPOS connectors, please consult the EPOS2 24/2 hardware reference.

Table A.8: Connector P101 on the calibration system PCB.

Pin	Signal	Description
1	UART Tx	IMU communication transmit (fused)
2	UART Rx	IMU communication receive (fused)
3	GND	IMU power and communication ground
4	12VDC	IMU motherboard power supply (fused)
5	GND	Power ground for middle and inner EPOS
6	24VDC	Power supply for middle and inner EPOS (fused)

Table A.9: Connector on inner gimbal.

Pin	Signal	Description
1	Not connected	Broken slip ring
2	UART Tx	IMU communication transmit
3	12VDC	IMU motherboard power supply
4	Not connected	Broken slip ring
5	UART Rx	IMU communication receive
6	GND	IMU power and communication ground

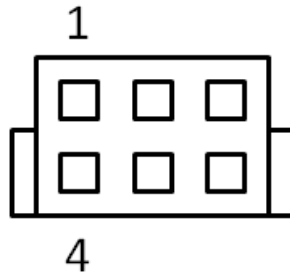


Figure A.6: Pin numbering of female connector on inner gimbal.

### A.6.5 Calibration System PCB

An overview of the calibration system's PCB is shown in figure A.7, the exact scheme of the PCB can be found in figure A.8 and a model of the actual routing in figure A.9.

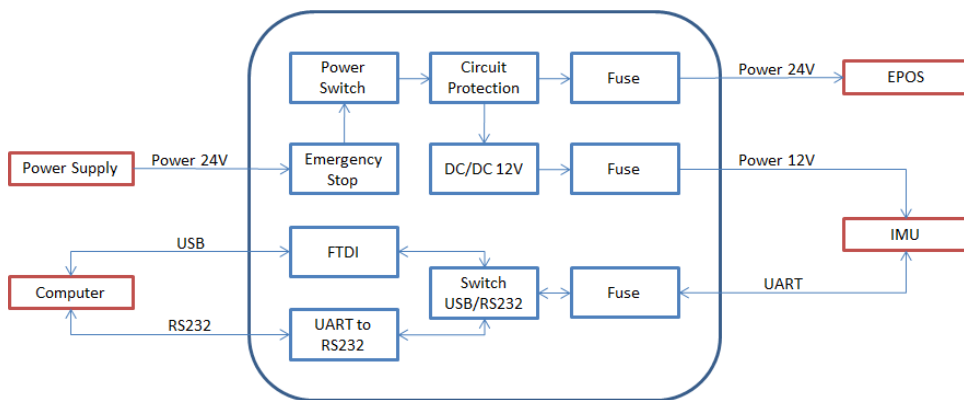


Figure A.7: Overview of the calibration system's PCB.

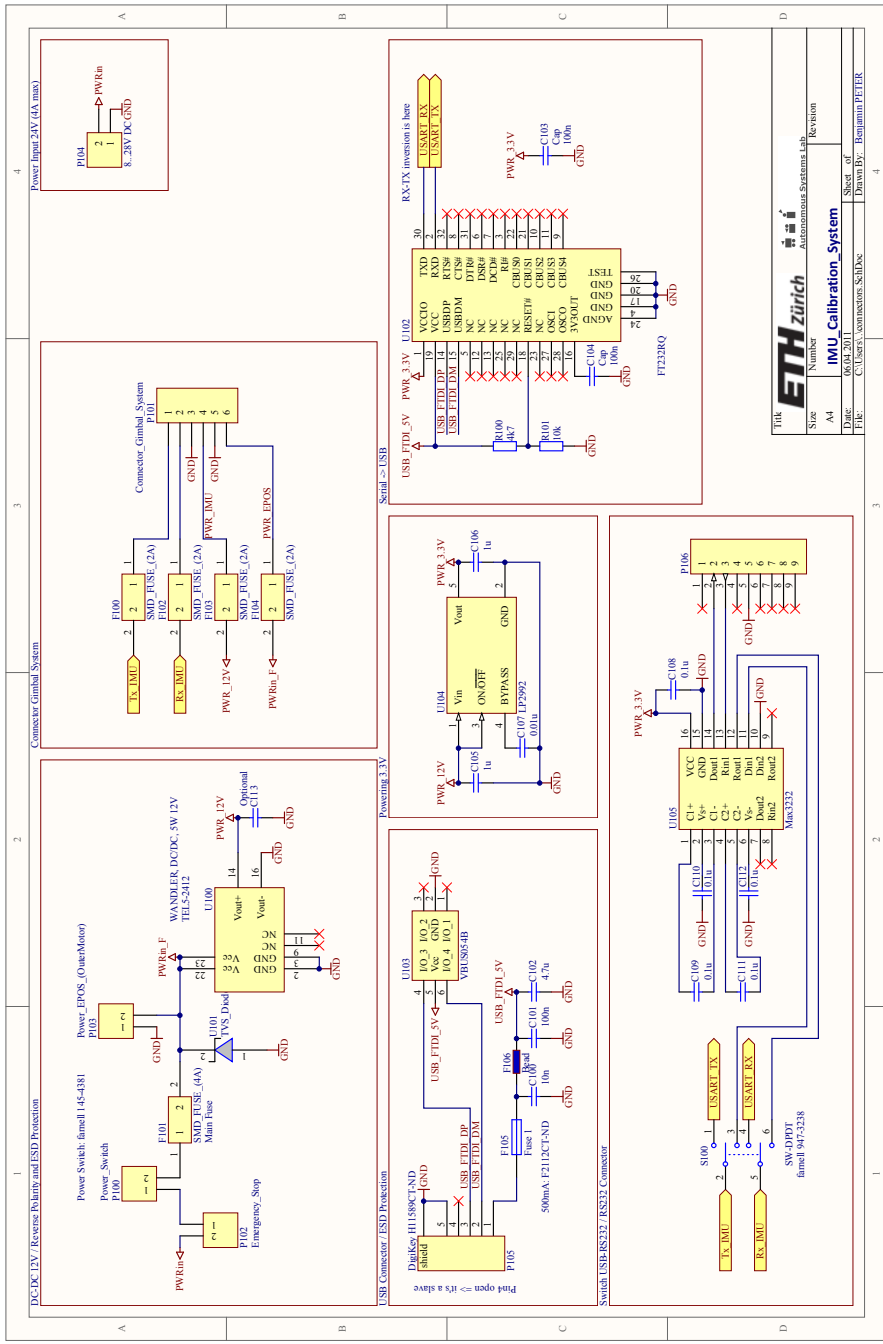


Figure A.8: Scheme of the calibration system's PCB.

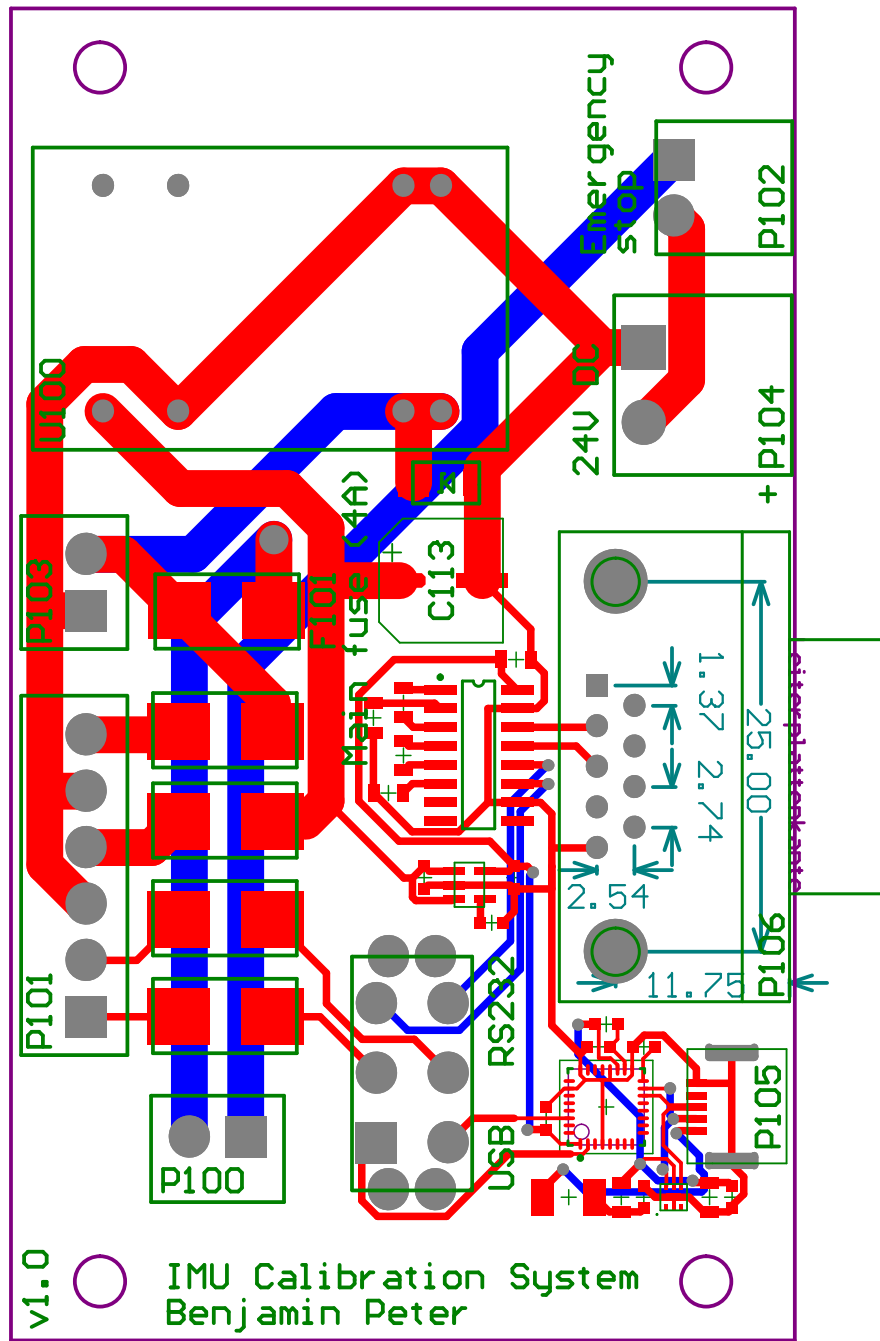


Figure A.9: Actual routing of the calibration system's PCB.

## A.7 Maintenance and Handling Remarks

### A.7.1 Lubrication

The spur gears in the base can be lubricated through the lubrication hole in the gear housing. The hole is normally covered by a screw to prevent particles from getting in and damaging the system. To lubricate the gears, apply grease on the teeth through the lubrication hole. Slowly rotate the outer gimbal for a full revolution in order to cover all teeth.

All bearings used are sealed and lubricated for their lifetimes.

### A.7.2 Springs

The counter-backlash torque can be adjusted by moving the spring attachment parts, further extending or collapsing the springs. Two opposing springs should be equally extended at all times to ensure a pure torque with no additional radial forces. The easiest way to equalise the spring lengths is to completely unwind the attachment string and wind it up again.

If desired, the springs can be removed entirely to allow unlimited rotation of the middle and inner gimbal. However, the positioning will be much less accurate.

### A.7.3 Removing Slip Rings

If a slip ring has to be removed, all strands located on the rotating side leading to this particular slip ring have to be cut. Thus, removing slip rings should be avoided if possible. When reattaching the slip ring, make sure that the strands on the rotating side are protected by shrink tubing and that the o-ring is in place. Otherwise, a cable break may occur during operation.

## Appendix B

### Part List

All milled and turned parts of the calibration system are shown in figure B.1. A list can be found in table B.1. CAD drawings of each part are depicted in figures B.2 through B.17.

Table B.1: List of milled and turned parts of the calibration system.

Part N°	Name	Quantity
1	Motor side of middle and inner shaft	2
2	Slip ring side of middle and inner shaft	2
3	Outer shaft	1
4	Base plate of the spur gear housing	1
5	Spur gear housing	1
6	Base column	1
7	Base plate	1
8	Outer gimbal	1
9	Middle gimbal	1
10	Inner gimbal	1
11	Motor controller mounting plate	2
12	IMU mounting plate	1
13	Motor mounting part	2
14	Slip ring mounting part	2
15	Water level attachment part	1
16	Spring attachment part	4

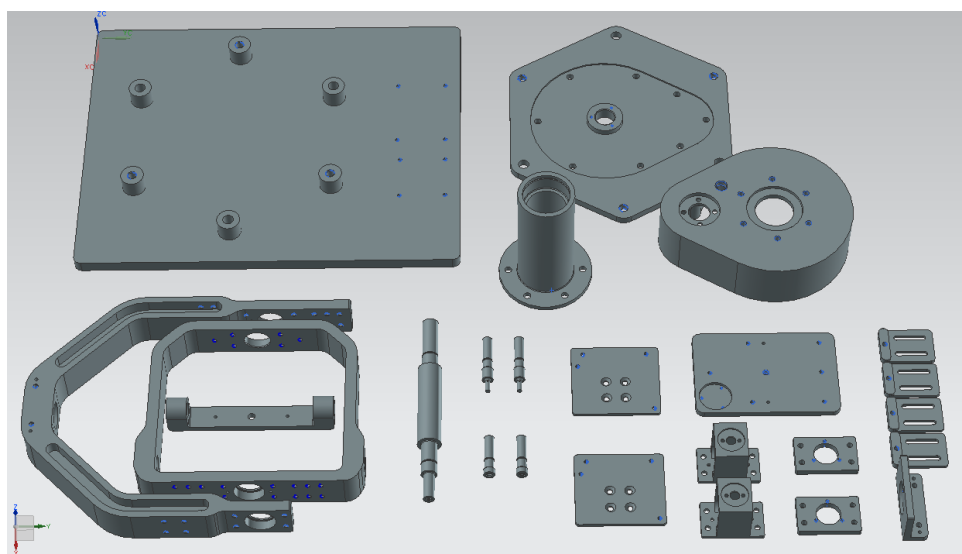


Figure B.1: CAD models of all the milled and turned parts of the calibration system.

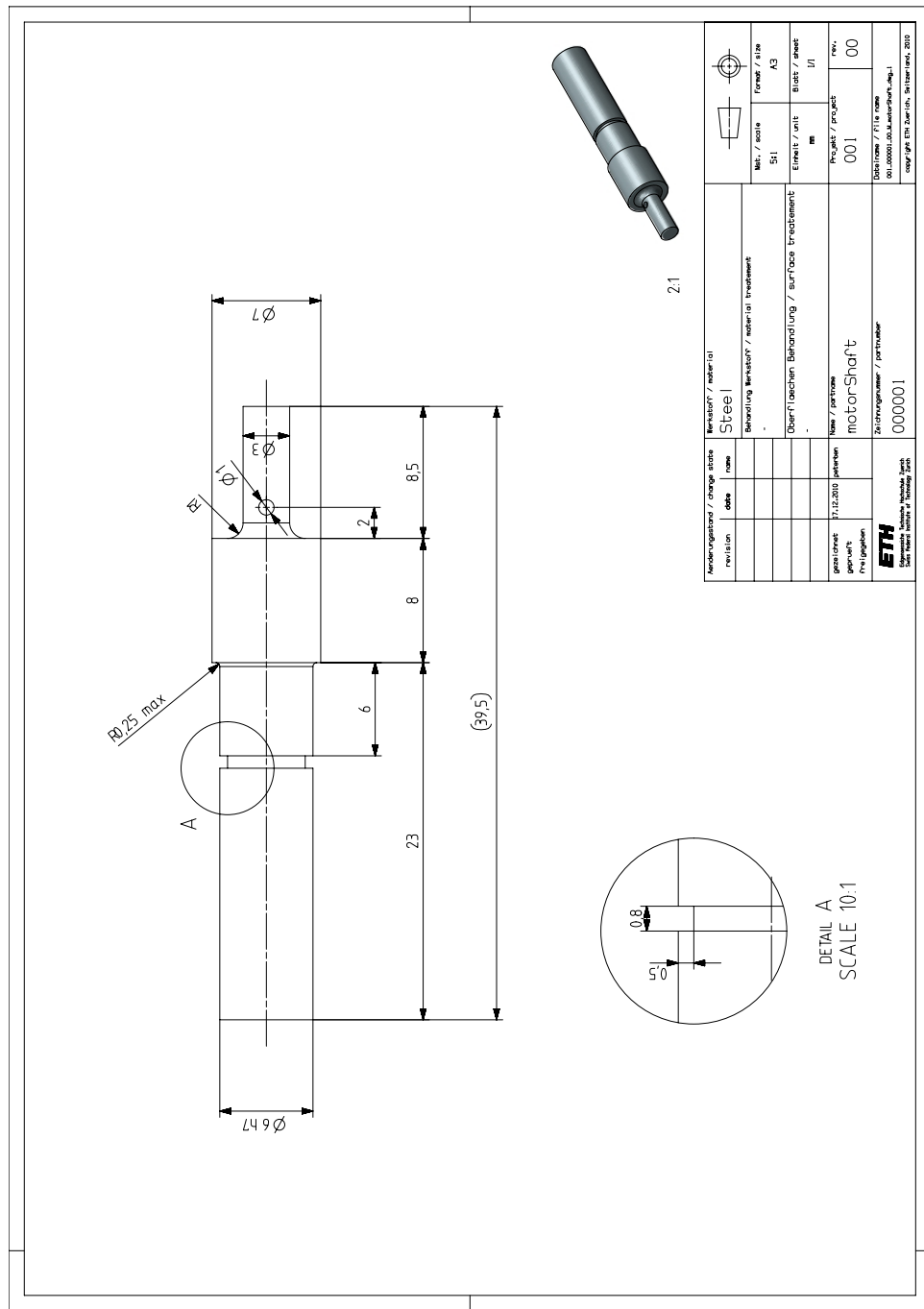


Figure B.2: Motor side of middle and inner shaft

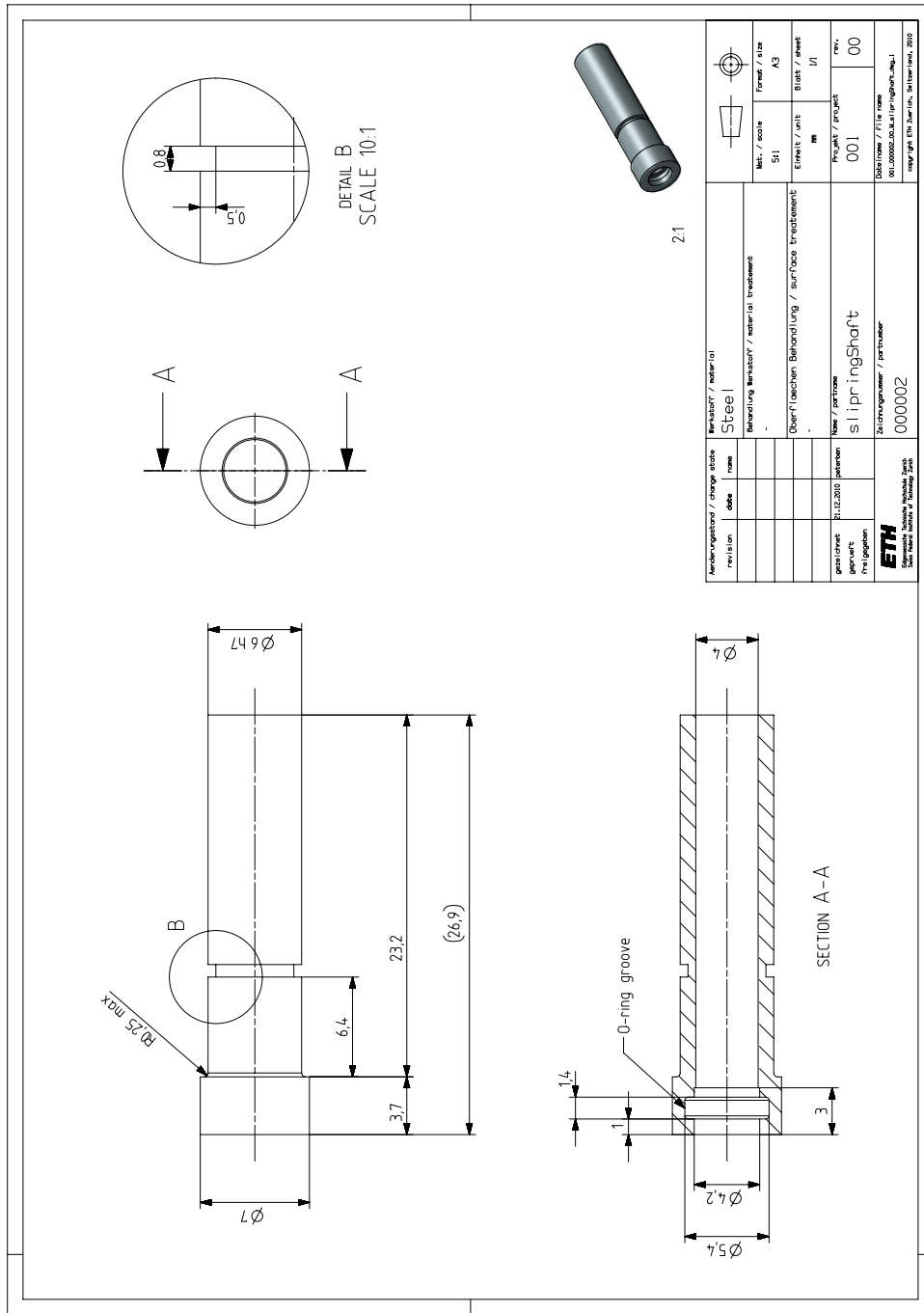


Figure B.3: Slip ring side of middle and inner shaft

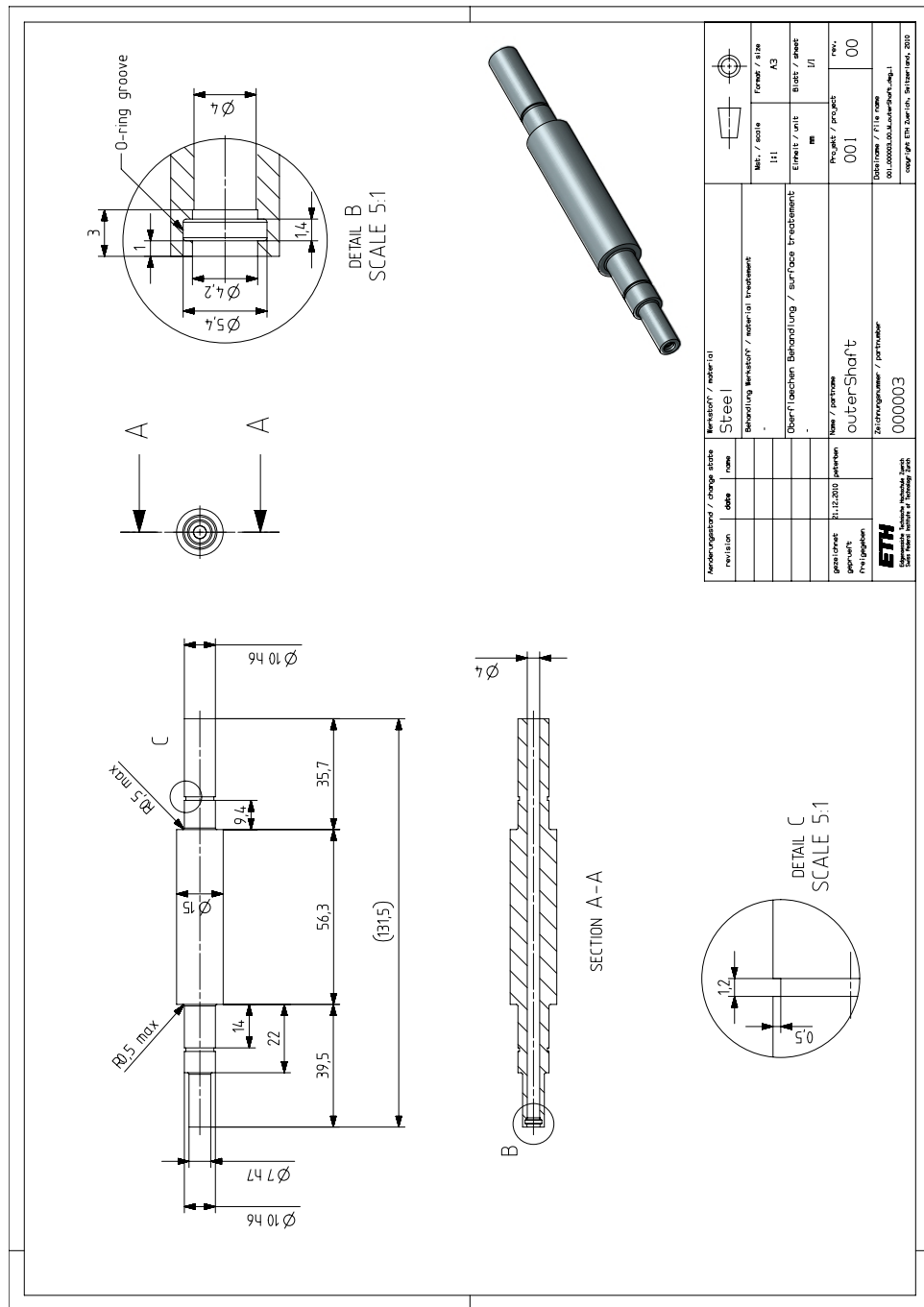


Figure B.4: Outer shaft

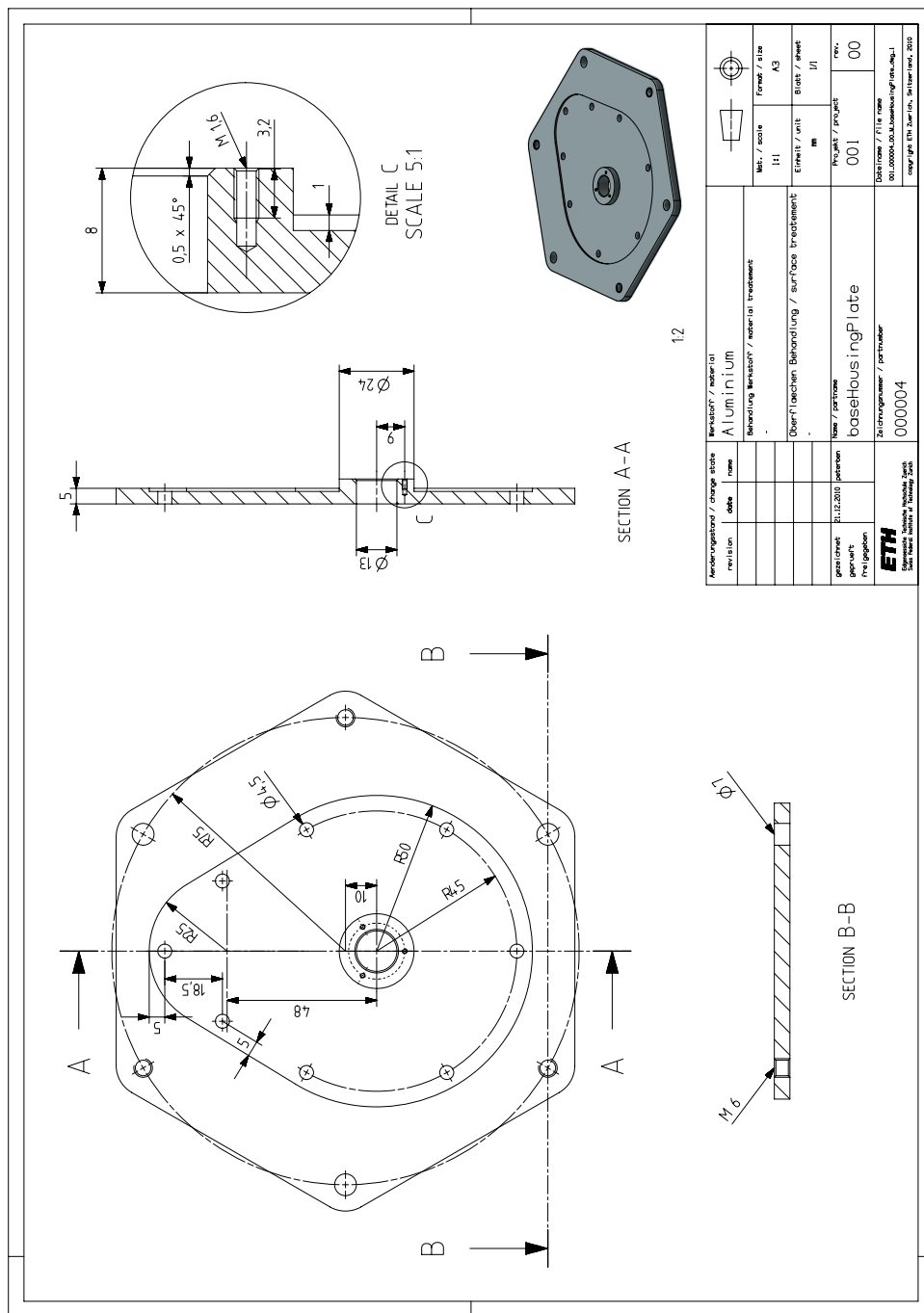


Figure B.5: Base plate of the spur gear housing

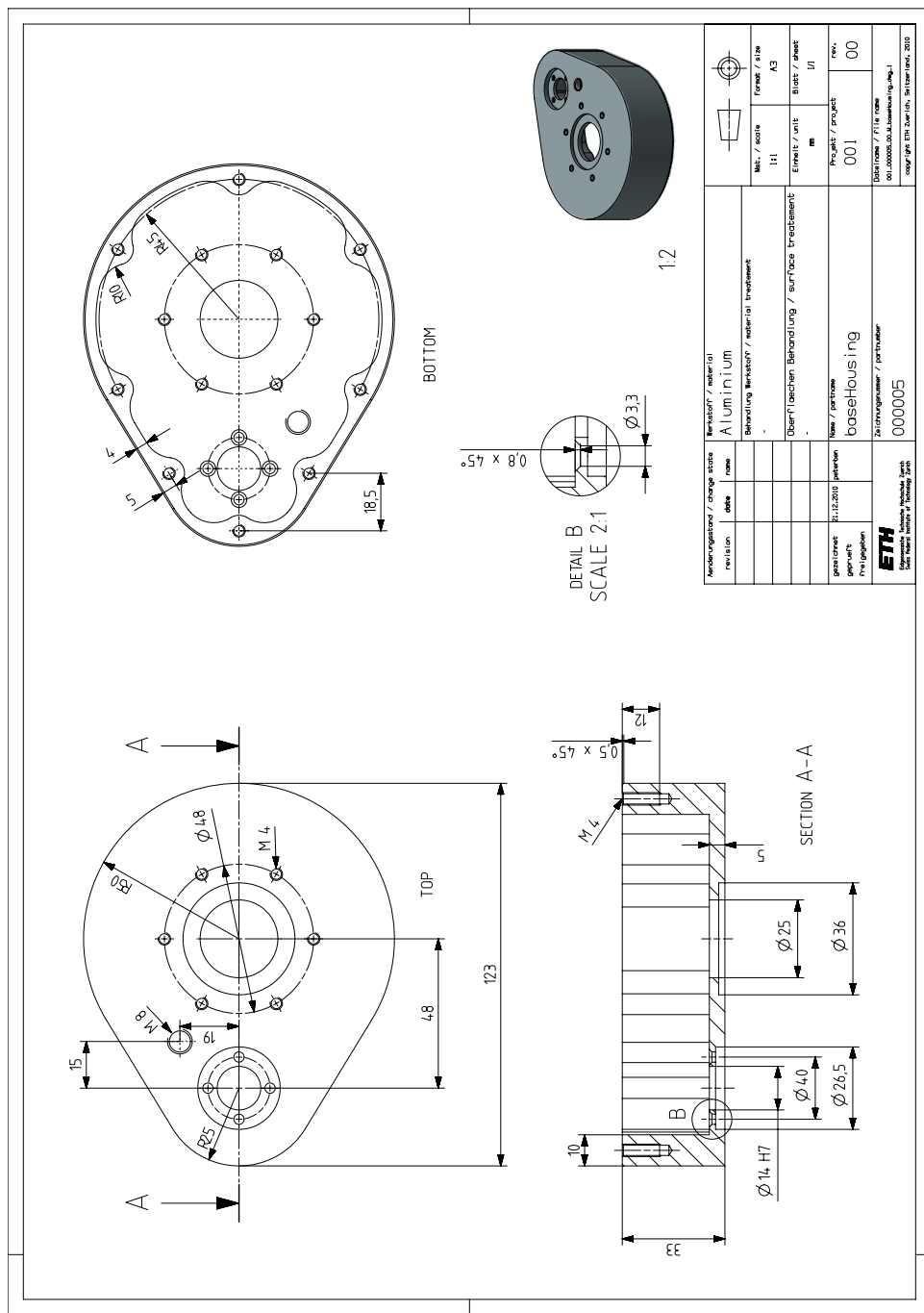


Figure B.6: Spur gear housing

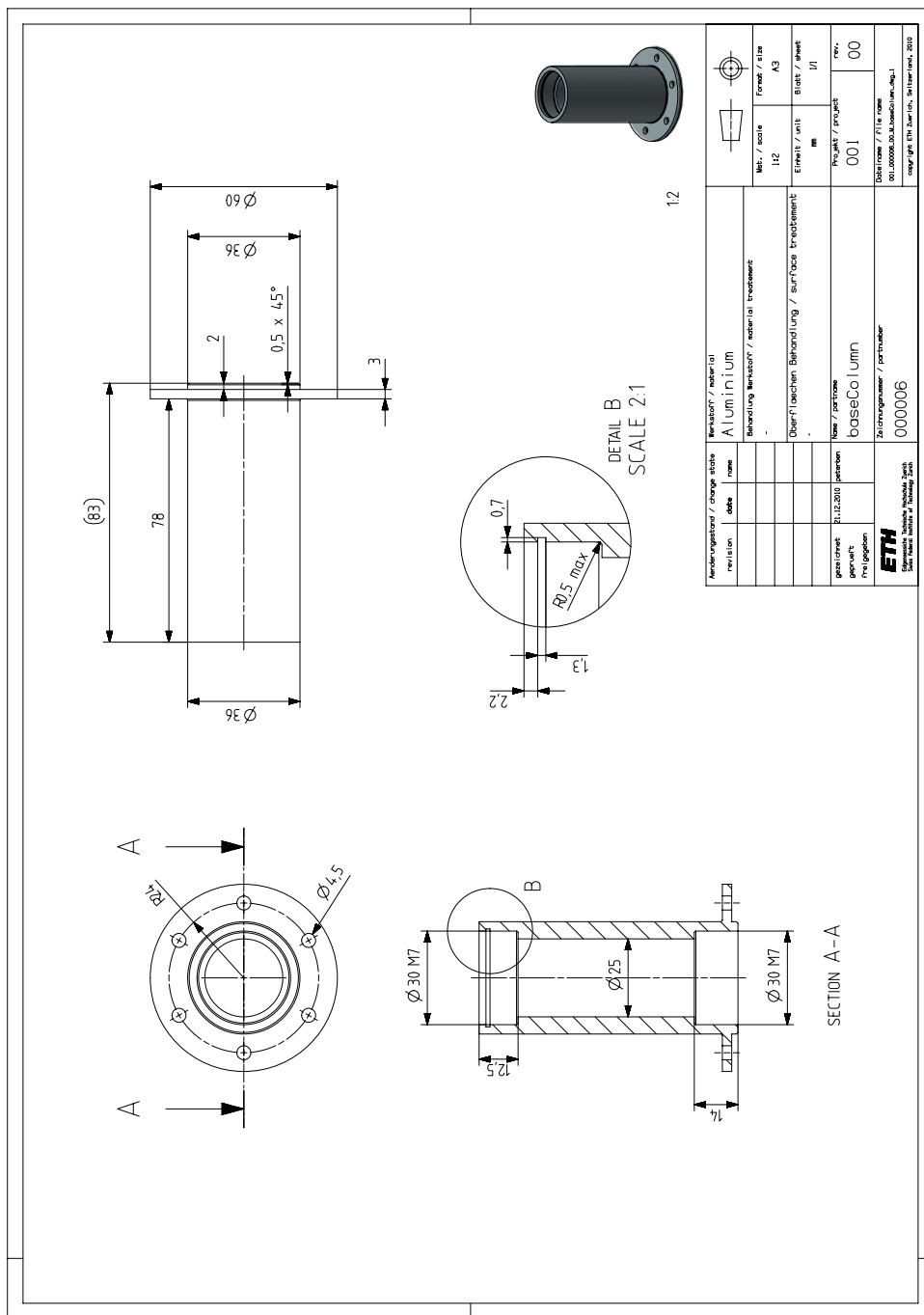


Figure B.7: Base column

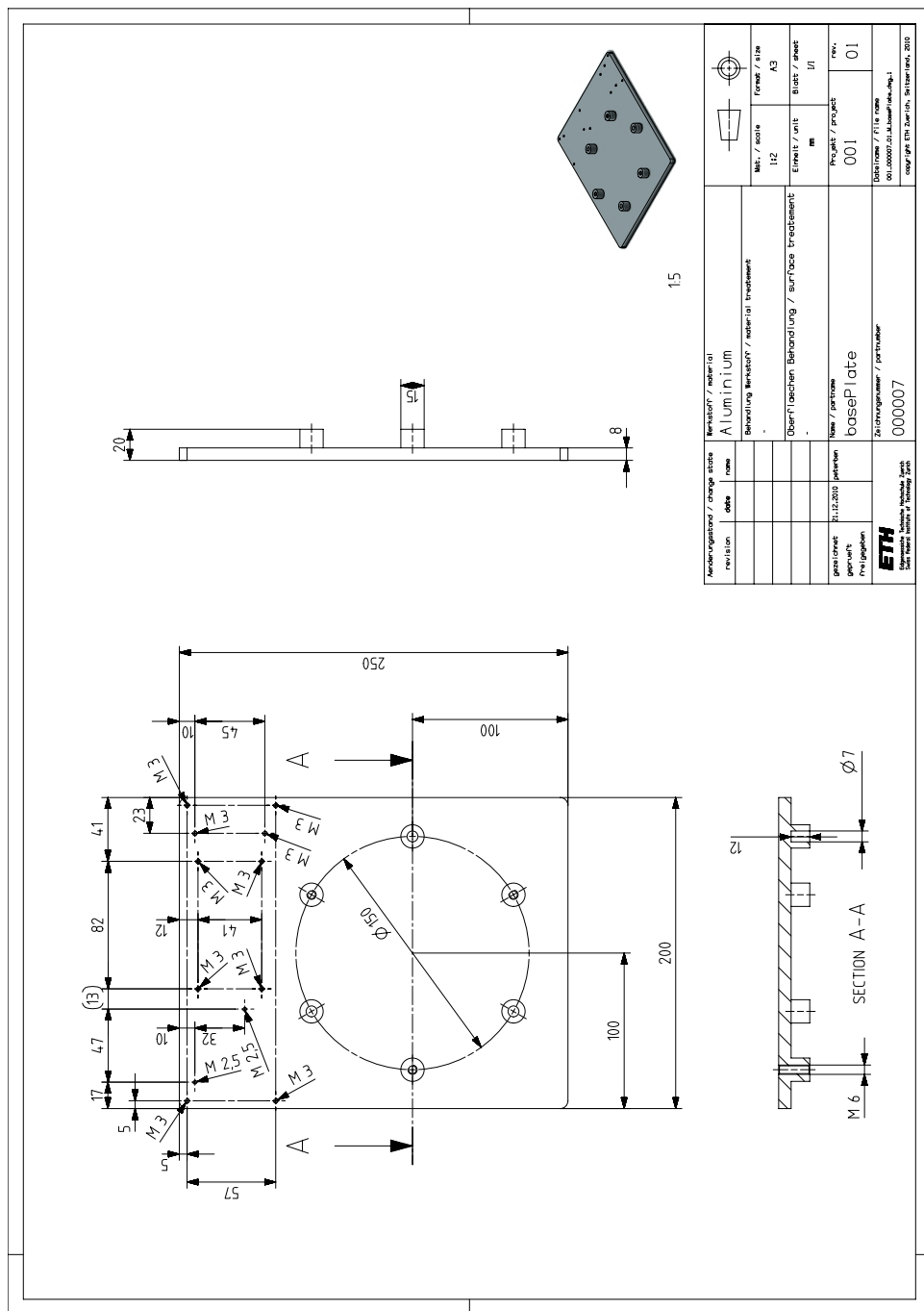


Figure B.8: Base plate

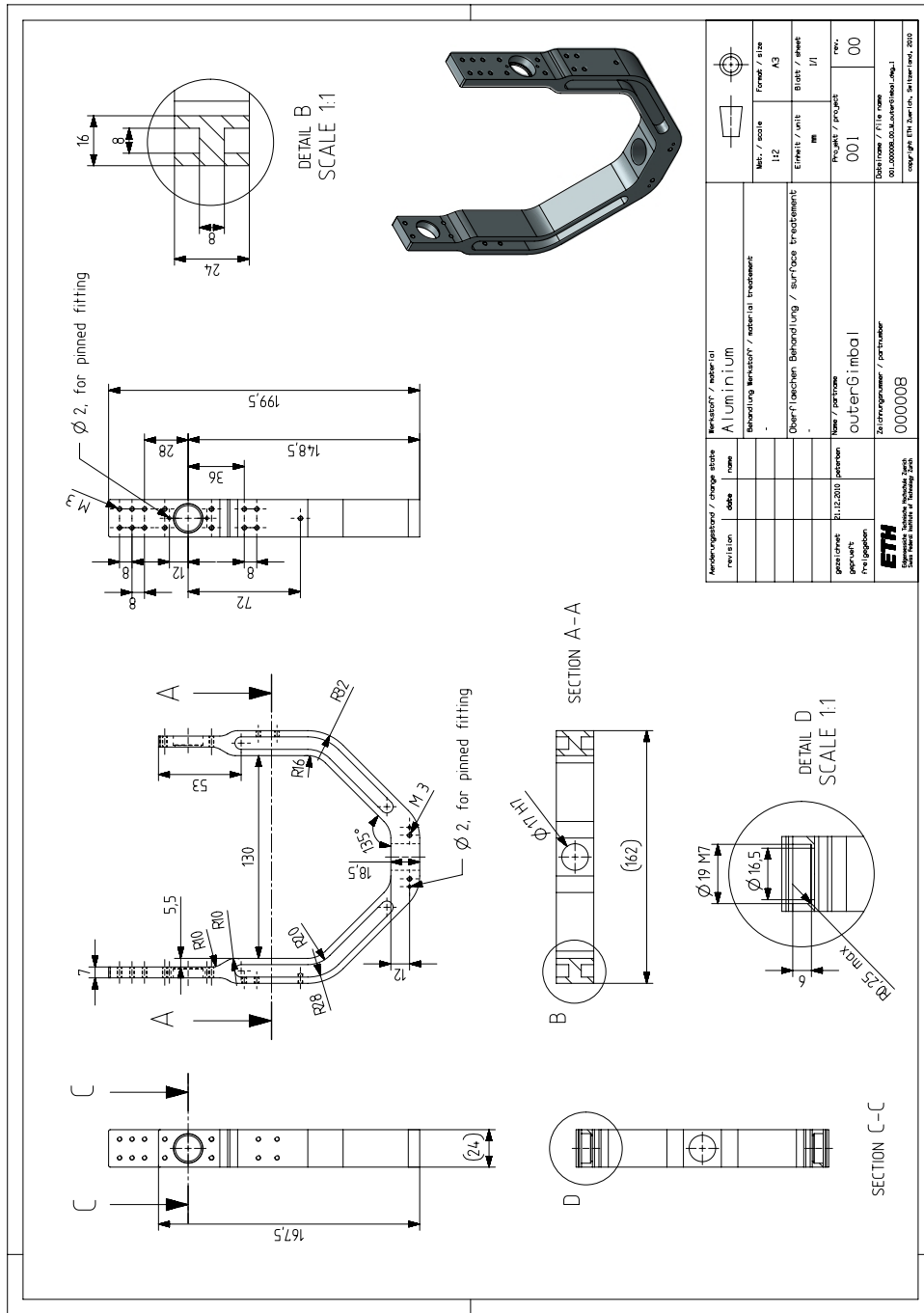


Figure B.9: Outer gimbal

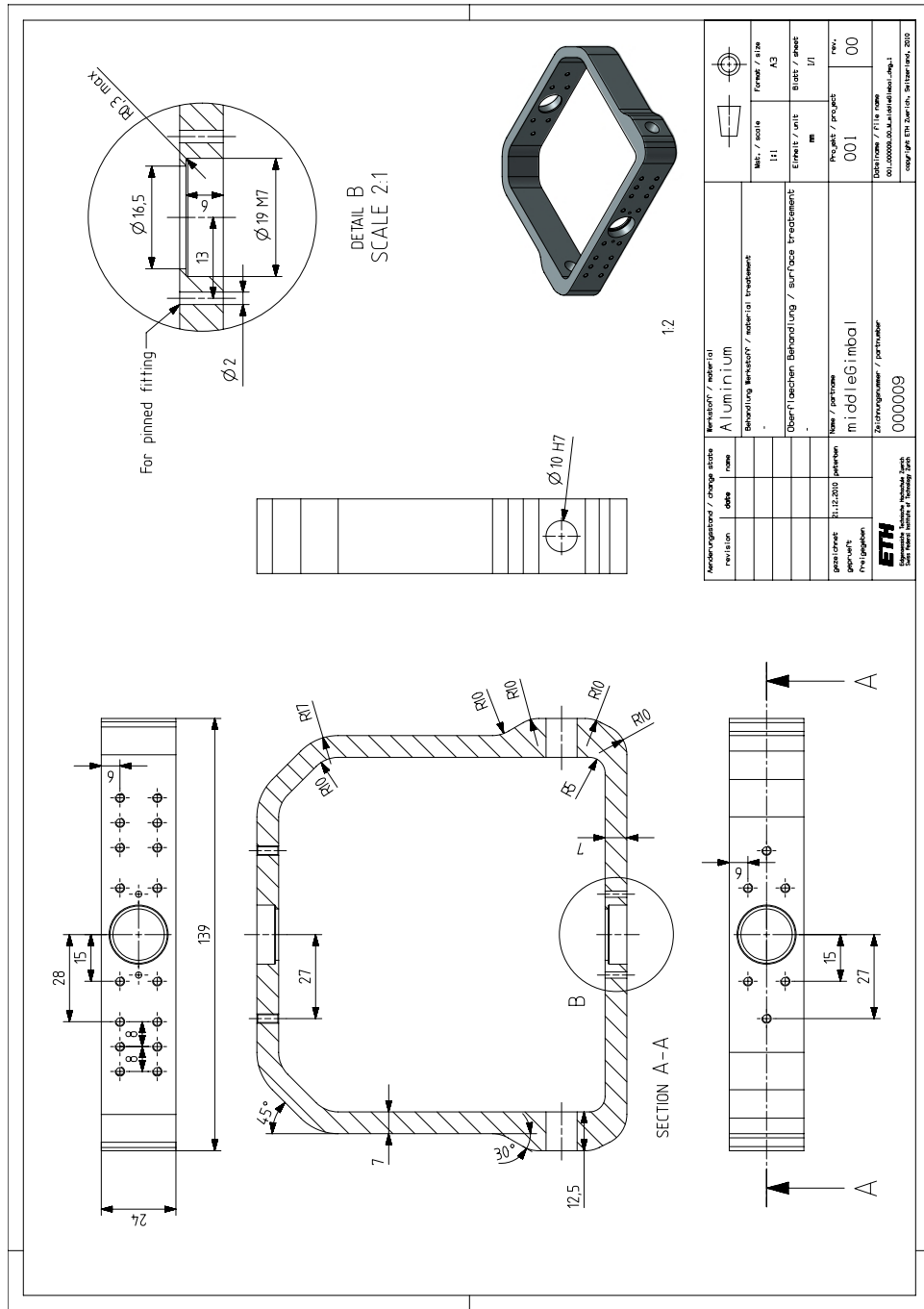


Figure B.10: Middle gimbal

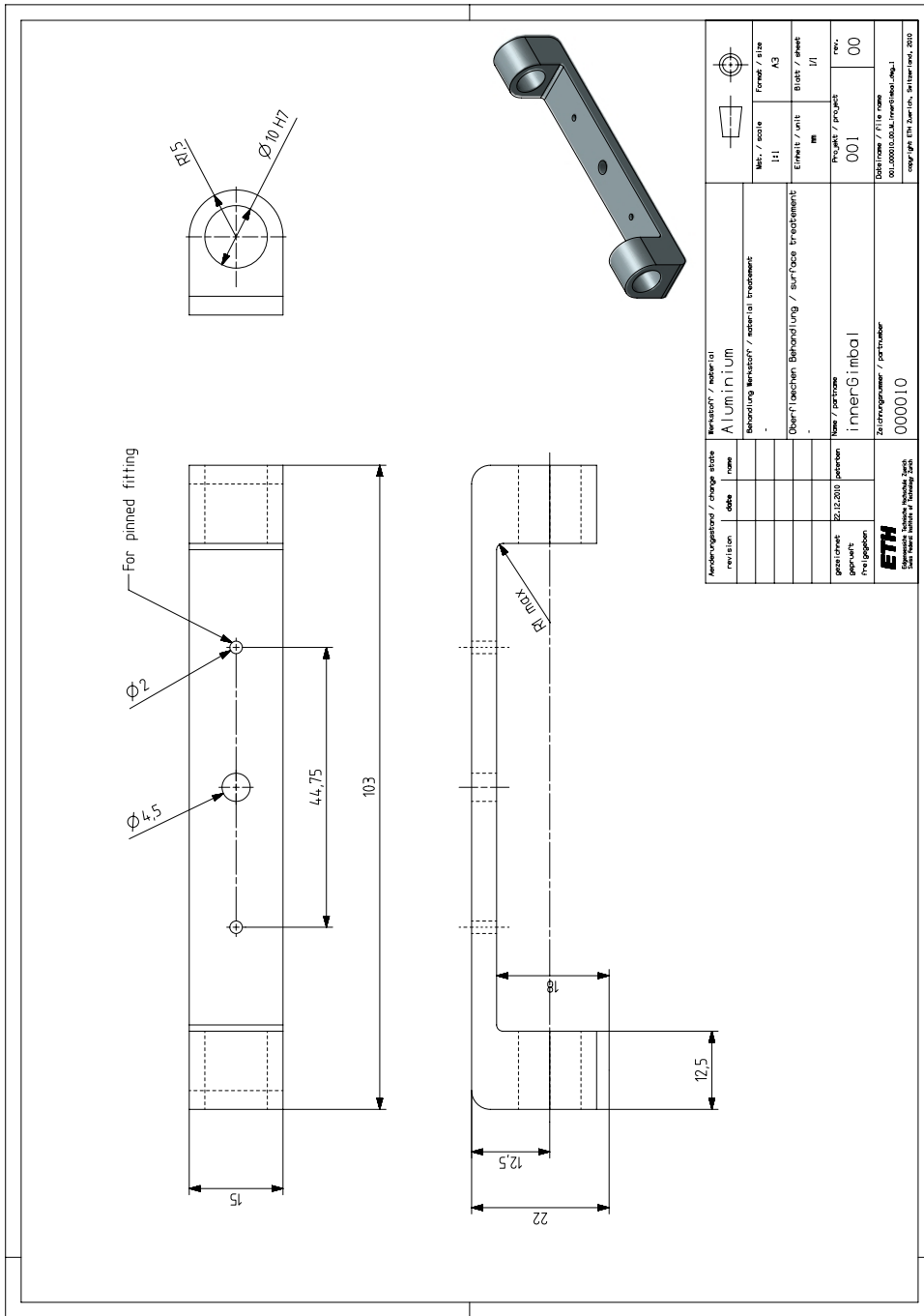


Figure B.11: Inner gimbal

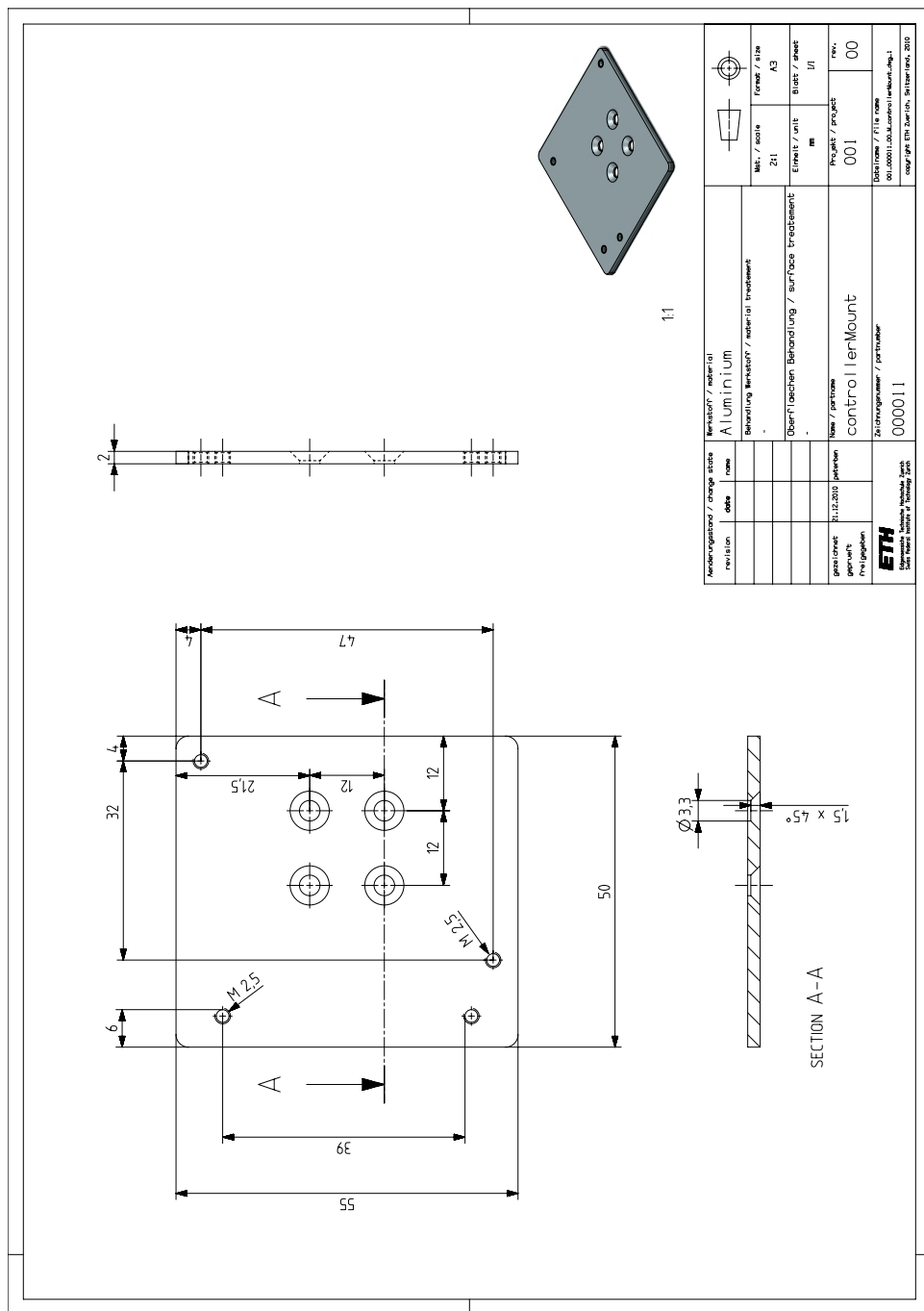


Figure B.12: Motor controller mounting plate

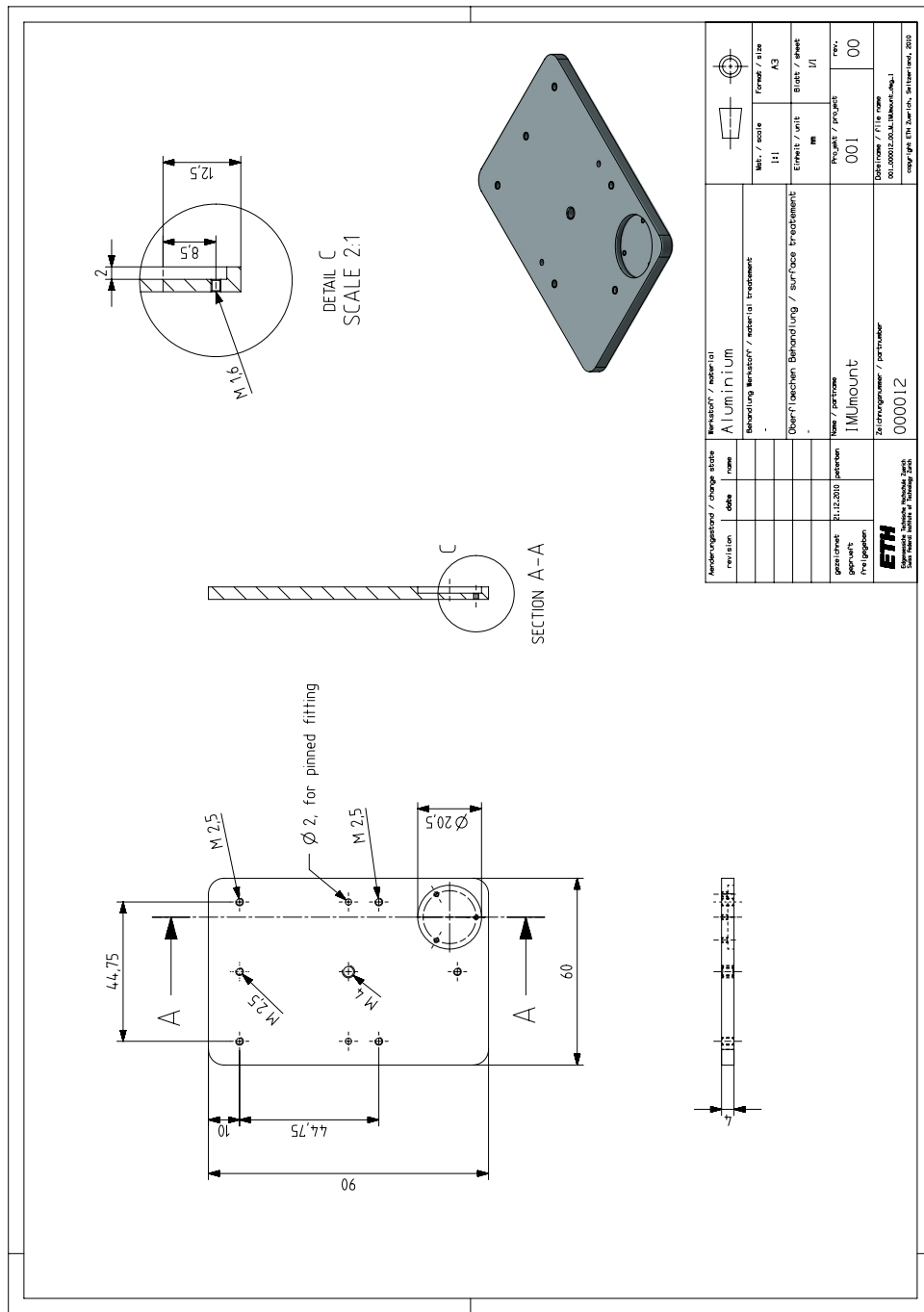


Figure B.13: IMU mounting plate

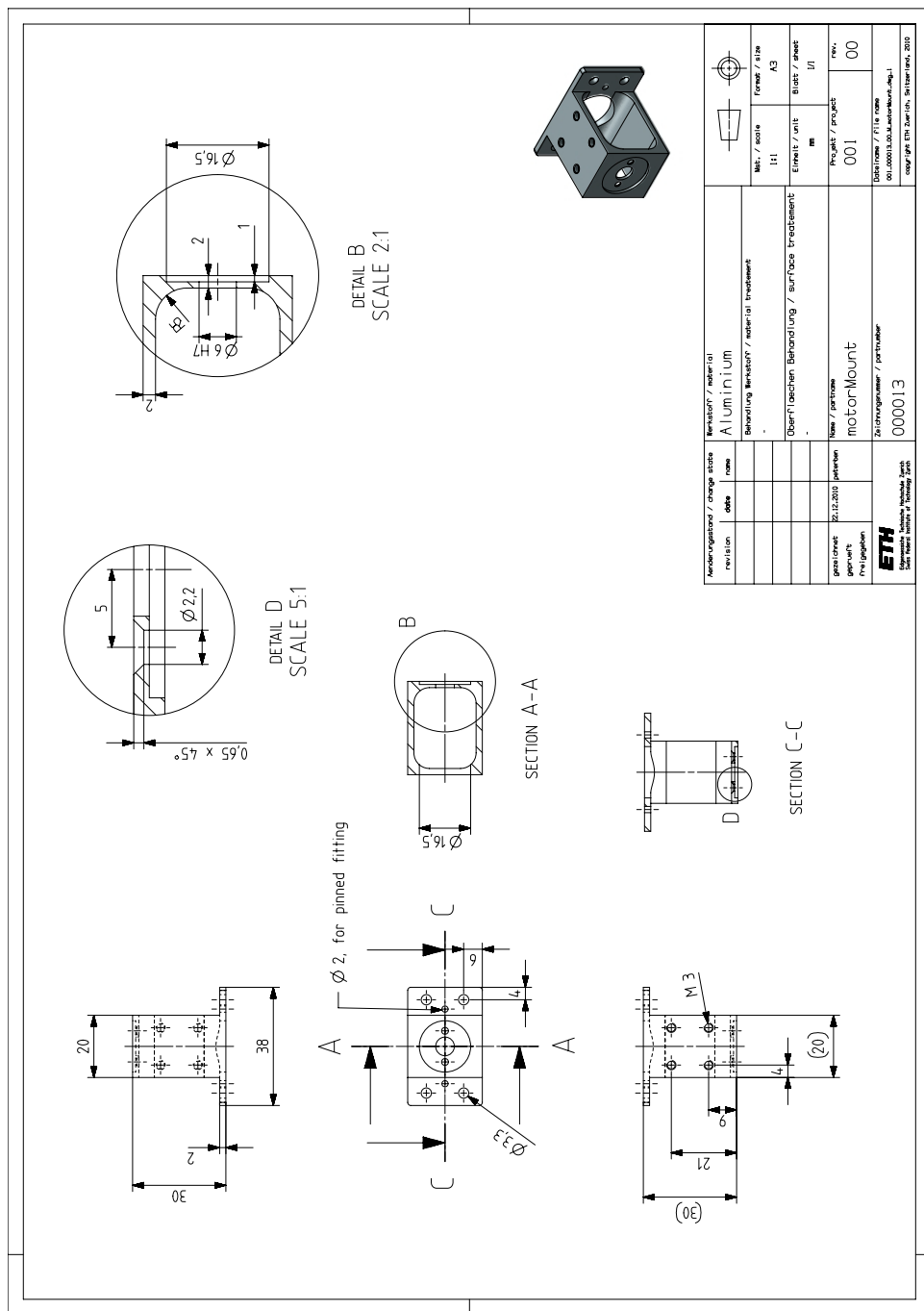


Figure B.14: Motor mounting part

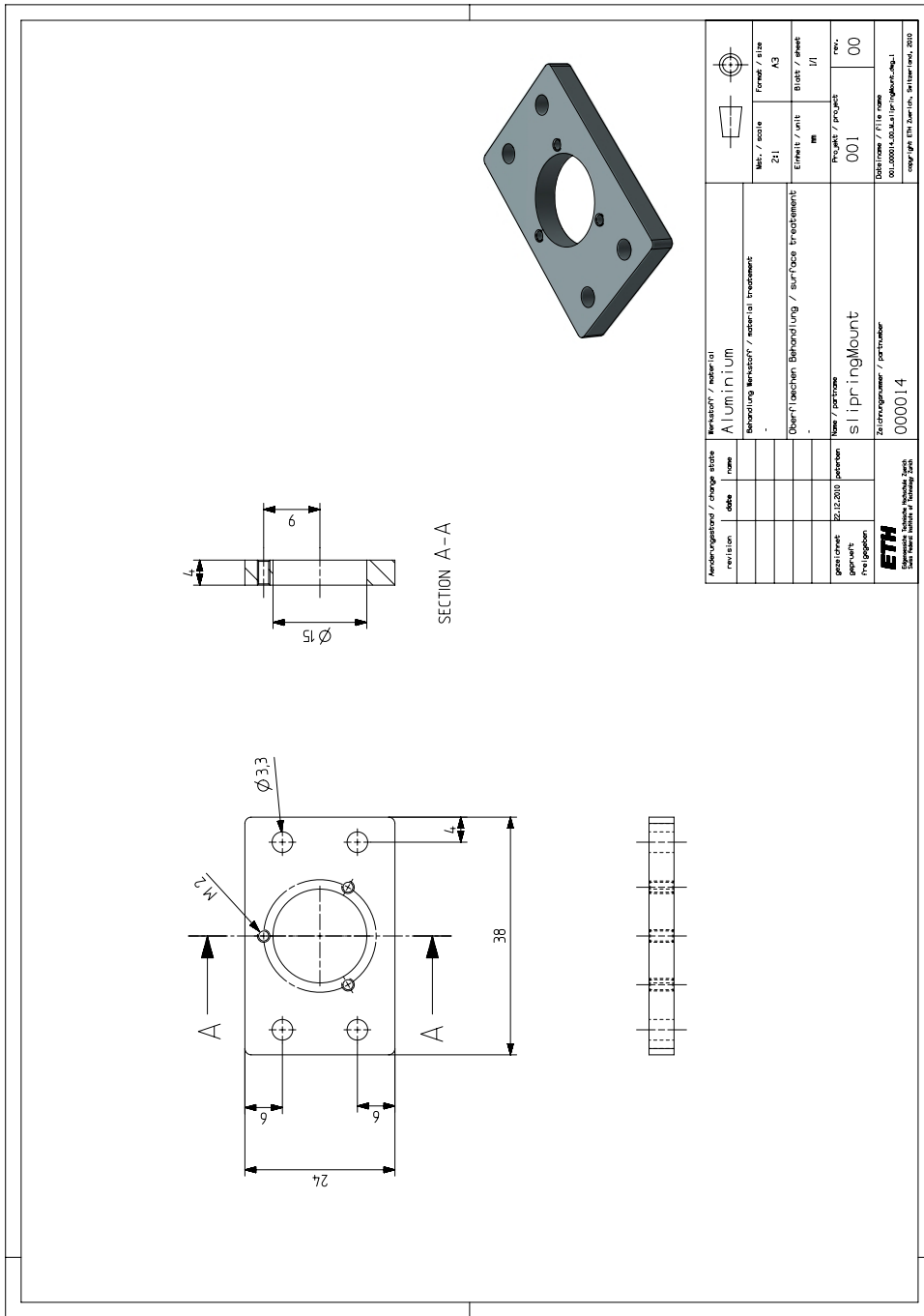


Figure B.15: Slip ring mounting part

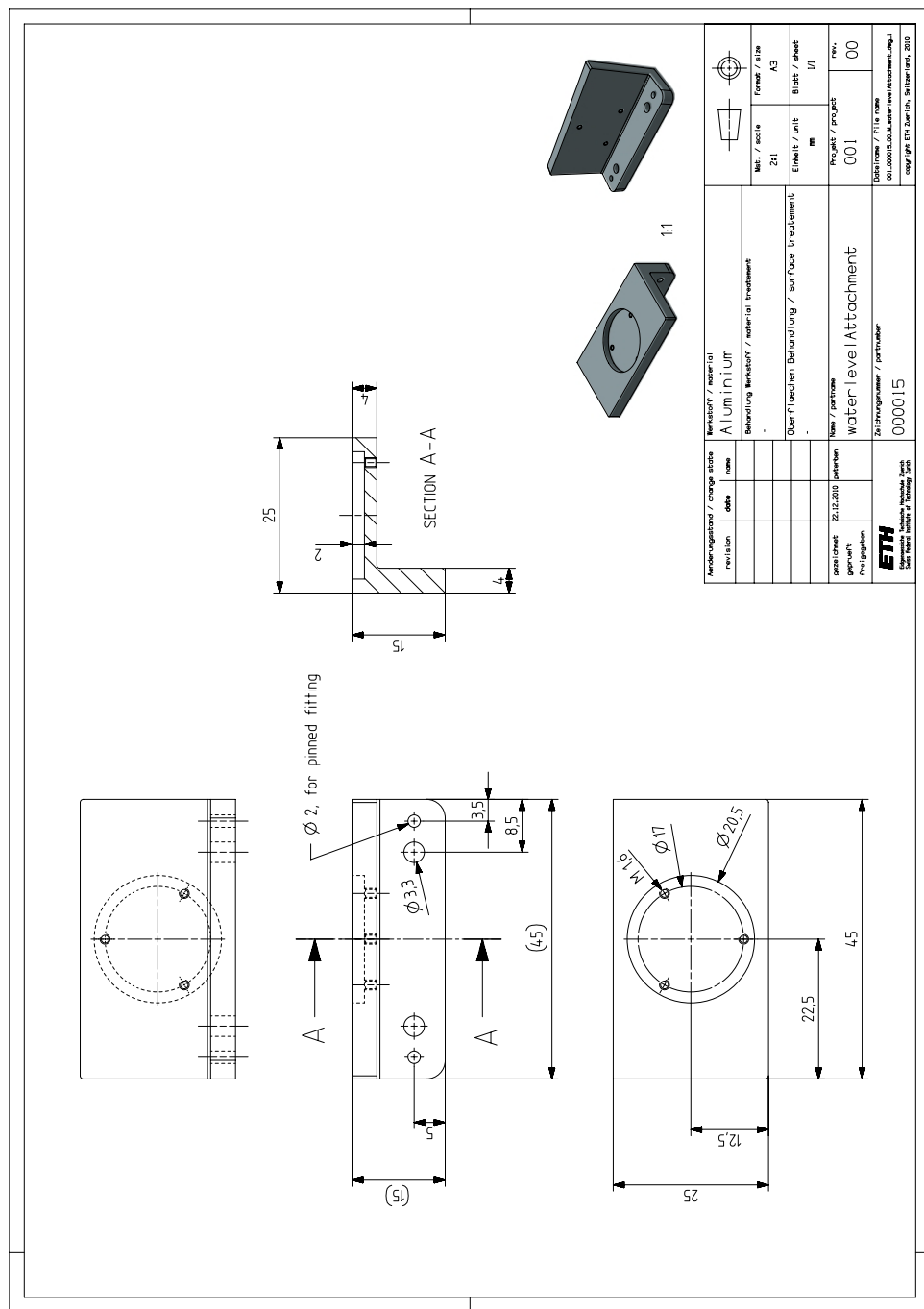


Figure B.16: Water level attachment part

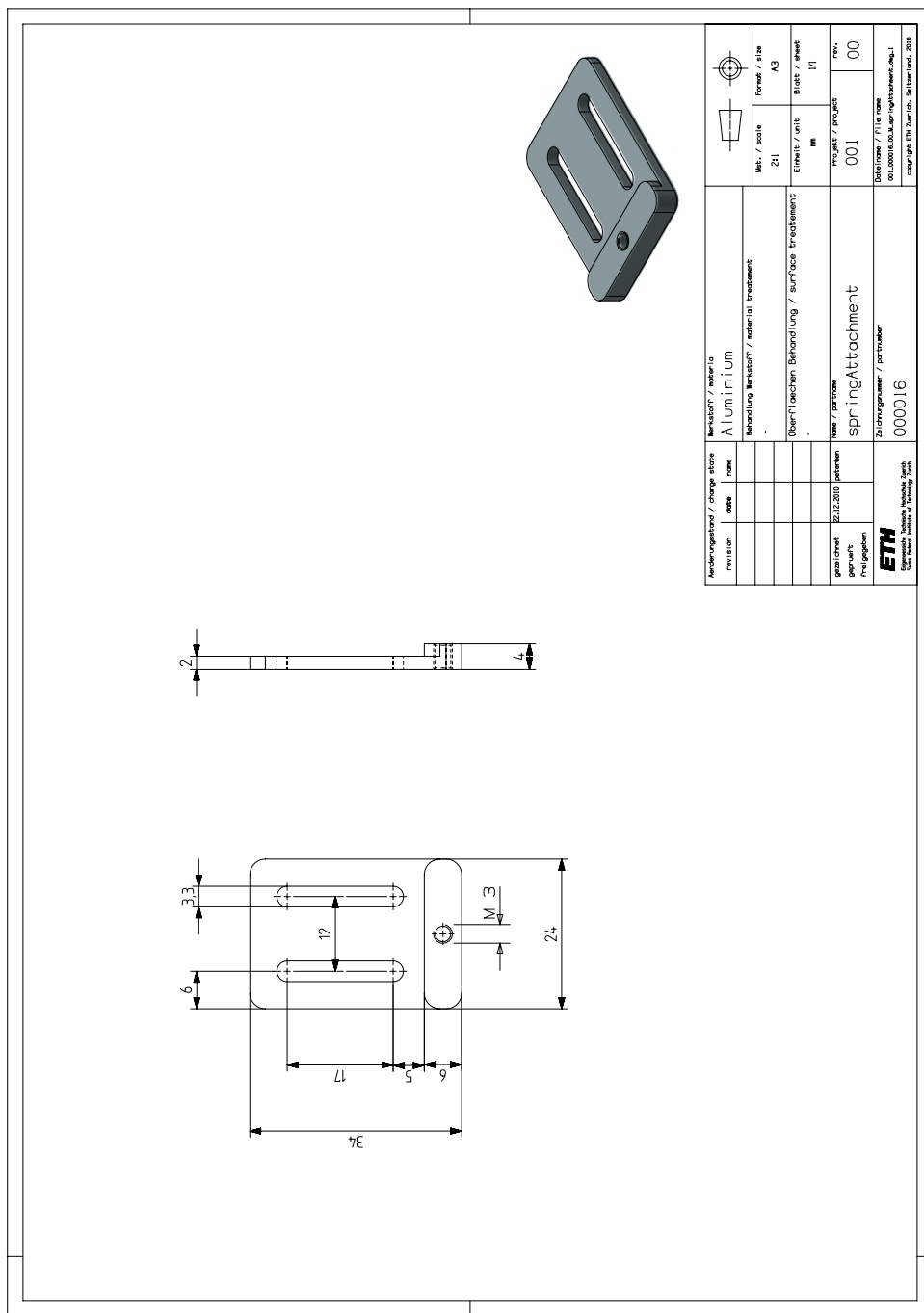


Figure B.17: Spring attachment part

# Bibliography

- [1] S. Fux. Development of a planar low cost Inertial Measurement Unit for UAVs and MAVs. Master's thesis, ETH Zurich, 2008.
- [2] Sebastian O.H. Madgwick. Automated calibration of accelerometers, magnetometers and gyroscopes - a feasabilit study, September 2010.
- [3] J.J. Hall, R.L. Williams II, and F. Grass. Inertial measurement unit calibration platform. *Journal of Robotic Systems*, 17(11):623–632, 2000.
- [4] J. Včelák, P. Ripka, J. Kubík, A. Platil, and P. Kašpar. AMR navigation systems and methods of their calibration. *Sensors and Actuators A: Physical*, 123:122–128, 2005.
- [5] M. Park. Error analysis and stochastic modeling of MEMS based inertial sensors for land vehicle navigation applications. *UCGE Report*, 20194:27–41, 2004.
- [6] A. Kim and MF Golnaraghi. Initial calibration of an inertial measurement unit using an optical position tracking system. In *Position Location and Navigation Symposium, 2004. PLANS 2004*, pages 96–101. IEEE, 2004.
- [7] A.B. Chatfield. *Fundamentals of High Accuracy Inertial Navigation*. AIAA (American Institute of Aeronautics & Astronautics), 1997.
- [8] J. Diebel. Representing attitude: Euler angles, unit quaternions, and rotation vectors, 2006.
- [9] I. Skog and P. Händel. Calibration of a MEMS Inertial Measurement Unit. In *XVII IMEKO World Congress on Metrology for a Sustainable Development, September*, pages 17–22. Citeseer, 2006.
- [10] MEMS IMU calibration example. Sentera Technology Corporation.
- [11] B. Schlecht. *Maschinenelemente 2: Getriebe, Verzahnungen und Lagerungen*. Pearson Education, 2009.